AMS Short Course on Rigorous Numerics in Dynamics: (Un)Stable Manifolds and Connecting Orbits

J.D. Mireles James, *

December 1, 2015

Abstract

The study of dynamical systems begins with consideration of basic invariant sets such as equilibria and periodic solutions. After local stability, the next important question is how these basic invariant sets fit together dynamically. Connecting orbits play an important role as they are low dimensional objects which carry global information about the dynamics. This principle is seen at work in the homoclinic tangle theorem of Smale, in traveling wave analysis for reaction diffusion equations, and in Morse homology.

This lecture builds on the validated numerical methods for periodic orbits presented in the lecture of J. B. van den Berg. We will discuss the functional analytic perspective on validated stability analysis for equilibria and periodic orbits as well as validated computation of their local stable/unstable manifolds. With this data in hand we study heteroclinic and homoclinic connecting orbits as solutions of certain projected boundary value problems, and see that these boundary value problems are amenable to an a posteriori analysis very similar to that already discussed for periodic orbits. The discussion will be driven by several application problems including connecting orbits in the Lorenz system and existence of standing and traveling waves.

Contents

*Florida Atlantic University. Email: jmirelesjames@fau.edu.

1 Introduction

These notes accompany the 2016 AMS short course on Rigorous Numerics in Dynamics lecture on invariant manifolds and connecting orbits. The goal is to present a functional analytic tool kit for mathematically rigorous computer assisted study of intersections of invariant manifolds for differential equations. We begin with a brief discussion of a functional analytic framework for computer assisted proof of transverse connecting orbits for diffeomorphisms, i.e. discrete time dynamical systems. This brief introductory discussion motivates the more detailed material in the remainder of the notes.

In Section 2 we discuss the Parameterization Method for invariant manifolds. In particular we discuss some techniques for computing high order Taylor and Fourier-Taylor approximations for stable/unstable manifolds for equilibria and periodic orbits of differential equations. One feature of these methods is that they are amiable to the kind of a-posteriori analysis discussed in the notes for the introductory lecture by J.B. van den Berg [1].

Finally, in Section 3 we discuss spectral methods for solving some boundary value problems which characterize connecting orbits between equilibria and periodic orbits for differential equations. The solutions of the boundary value problems are represented as Chebeyshev series, and again the numerical computations can be validated via a-posteriori analysis similar to that discussed in [1].

1.1 A motivating example: heteroclinic orbits for diffeormophisms

These notes discuss a functional analytic approach to computer assisted study of connecting orbits for dynamical systems. In order to motivate the presentation we first introduce the ideas in a simplified context.

Let $f\colon \mathbb{R}^N \to \mathbb{R}^N$ be a diffeomorphism and $x_0 \in \mathbb{R}^N$. Define the *sequence of forward iterates of* x_0 by

$$\begin{aligned} x_1 &= f(x_0) \\ x_2 &= f(x_1) \\ &\vdots \\ x_{n+1} &= f(x_n) \end{aligned}$$

for all $n \in \mathbb{N}$ and the *sequences of backward iterates of* x_0 by

$$\begin{aligned} x_{-1} &= f^{-1}(x_0) \\ x_{-2} &= f^{-2}(x_{-1}) \\ &\vdots \\ x_{-(n+1)} &= f^{-1}(x_{-n}) \end{aligned}$$

for all $n \in \mathbb{N}$. The union of these sequences is called the orbit of x_0 and we write

$$\text{orbit}(x_0) = \{x_n\}_{n=0}^{\infty} \cup \{x_{-n}\}_{n=0}^{\infty}.$$

The discussion is simplified by writing

$$x_n = f^n(x_0),$$

where for $n > 0$ f^n denotes the composition of f with itself n times, for $n < 0$ f^n denotes the composition of f^{-1} with itself n times, and when $n = 0$ f^n simply denotes the identity map. In this notation we have simply that

$$\text{orbit}(x_0) = \{f^n(x_0)\}_{n \in \mathbb{Z}}.$$

Now let $p, q \in \mathbb{R}^N$ denote a pair of fixed points for the map f, i.e. suppose that

$$f(p) = p, \qquad \text{and} \qquad f(q) = q.$$

We are interested in *connecting orbits* from p to q. To be precise we make the following definition: let $x_0 \in \mathbb{R}^N$ be a third and distinct point from p and q. We say that the orbit of x_0 is heteroclinic from p to q if

$$\lim_{n \to \infty} f^n(x_0) = p, \qquad \text{and} \qquad \lim_{n \to \infty} f^{-n}(x_0) = q.$$

We refer to the orbit of x_0 as a heteroclinic connection or heteroclinic connecting orbit. If $p = q$ we say that the orbit is homoclinic for p.

Now we are interested in formulating an analytic characterization of a heteroclinic connecting orbit. To do this we consider the unstable and stable manifolds of the fixed points. More precisely, suppose that $q \in \mathbb{R}^N$ a hyperbolic fixed point of f, i.e. we assume that that $Df(q)$ has no eigenvalues on the unit circle. Let $N_s \leq N$ denote the number of stable eigenvalues of $Df(q)$. Now for any open neighborhood $U \subset \mathbb{R}^N$ containing q the local stable manifold of q relative to U is defined to be the set

$$W^s_{\text{loc}}(q, U) := \left\{ x \in \mathbb{R}^N : \, q \in U \, \text{ and } f^n(q) \in U \text{ for all } n \geq 0 \right\}.$$

For a hyperbolic fixed point, the stable manifold theorem gives that there exists an $r > 0$ so that

- The local stable manifold $W^s_{\text{loc}}(q, B_r(q))$ is a smooth, embedded, N_s dimensional disk.
- $W^s_{\text{loc}}(q, B_r(q))$ is tangent to the stable eigenspace of $Df(q)$ at q.
- If $x \in W^s_{\text{loc}}(q, B_r(q))$ then
$$\lim_{n \to \infty} f^n(x) = q.$$

These considerations applied to f^{-1} at q give a local unstable manifold $W^u_{\text{loc}}(q)$ at q with analogous definition. Note that these local stable and unstable manifolds are not unique. However the sets

$$W^s(q) = \bigcup_{n=0}^{\infty} f^{-n}\left[W^s_{\text{loc}}(q)\right] = \left\{x \in \mathbb{R}^N \mid f^n(x) \to q \text{ as } n \to \infty\right\}$$

and

$$W^u(p) = \bigcup_{n=0}^{\infty} f^{n}\left[W^u_{\text{loc}}(p)\right] = \left\{x \in \mathbb{R}^N \mid f^{-n}(x) \to p \text{ as } n \to \infty\right\},$$

define uniquely a pair of globally invariant manifold (which however may no longer be immersed disks).

We now consider a pair of hyperbolic fixed points $p, q \in \mathbb{R}^N$, and let N_u and N_s denote the number of unstable eigenvalues of $Df(p)$ and the number of stable eigenvalues of $Df(q)$ respectively.

Via the definitions of the stable and unstable manifold, a heteroclinic orbit x_0 from p to q is characterized as a point

$$x_0 \in W^u(p) \cap W^s(q),$$

i.e. a point x_0 is heteroclinic from p to q if and only if x_0 is in the intersection of the stable and unstable manifolds.

We now write simply W^u_{loc} and W^s_{loc} to denote the local unstable and stable manifolds at p and q respectively. Since W^u_{loc} and W^s_{loc} are smooth manifolds there are neighborhoods $B_{r_u}(0) \subset \mathbb{R}^{N_u}$, $B_{r_s}(0) \subset \mathbb{R}^{N_s}$, and chart maps

$$P \colon B_{r_u}(0) \to \mathbb{R}^N \qquad Q \colon B_{r_s}(0) \to \mathbb{R}^N,$$

having

$$P(0) = p, \qquad Q(0) = q,$$

and

$$P(B_{r_u}(0)) \subset W^u_{\text{loc}}, \qquad Q(B_{r_s}(0)) \subset W^s_{\text{loc}}.$$

Moreover P and Q are tangent respectively to the unstable and stable eigenspaces of $Df(p)$ and $Df(q)$. Then in fact the images of P and Q are themselves local unstable and stable manifolds at p and q.

We now have that there exist $K_1, K_2 \in \mathbb{N}$, $\theta \in B_{r_u}(0)$ and $\phi \in B_{r_s}(0)$ so that

$$f^{K_1}(P(\theta)) = x_0,$$

and

$$f^{-K_2}(Q(\phi)) = x_0.$$

Letting $K = K_1 + K_2$ we see that this is

$$f^K(P(\theta)) = Q(\phi), \tag{1}$$

after applying f to x_0 K_2 times. For computational purposes Equation (1) is numerically unstable (for example when using interval arithmetic compositions introduce the so called "wrapping effect"). In order to stabilize the problem we introduce the additional variables x_1, x_2, …, x_K, defined by

$$\begin{aligned} P(\theta) &= x_1 \\ f(x_1) &= x_2 \\ &\vdots \\ f(x_{K-1}) &= x_K \\ f(x_K) &= Q(\phi) \end{aligned}$$

A solution $(\theta, x_1, \ldots, x_K, \phi)$ of this system of equations gives rise to a heteroclinic orbit from p to q. We observe that if $N_s + N_u = N$, then the equations above give a ballanced system of $N(K+1)$ scalar equations in $N(K+1)$ scalar unknowns. From now on we assume explicitly that $N_s + N_u = N$.

Inspired by these observations, define define the mapping $F\colon \mathbb{R}^{N(K+1)} \to \mathbb{R}^{N(K+1)}$ given by

$$F(\theta, x_1, \ldots, x_K, \phi) := \begin{pmatrix} P(\theta) - x_1 \\ f(x_1) - x_2 \\ \vdots \\ f(x_{K-1}) - x_K \\ f(x_K) - Q(\phi) \end{pmatrix}. \tag{2}$$

Then zeros of Equation (2) correspond to heteroclinic connections from p to q in the sense that if $(\hat{\theta}, \hat{x}_1, \ldots, \hat{x}_K, \hat{\phi})$ is a zero of F, then orbit(x_j) for $1 \leq j \leq K$ is a heteroclinic orbit from p to q. We call F *the connecting orbit operator*.

Remark 1.1.

- The equation $F(x) = 0$ given by Equation (2) can be studied via a numerical Newton method. This approach was introduced by Beyn in [2], and is sometimes called *the method of projected boundaries*. The name is reminiscent of the fact that the problem of finding a connecting orbit (a problem involving infinite forward and backward time asymptotics) is reduced to the problem of studying a finite orbit segment. This by "projecting" the orbit segment onto the local unstable and stable manifolds.

- Once a numerical approximate zero $\bar{x} \in \mathbb{R}^{N(K+1)}$ is found, we prove the existence of a true zero nearby using the mathematically rigorous a-posteriori analysis discussed in [1]. More precisely, one applies the contraction mapping theorem to the associated Newton-like operator
$$T(x) = x - AF(x),$$
in a neighborhood of the approximation x_0. Here A is a numerical approximate inverse for the matrix $DF(x_0)$. The interested reader can for example consult [3] for the details and implmentation.

- In [3] it is further shown that, under the assumption $N_s + N_u = N$, the connecting orbit operator F has a non-degenerate zero at $\hat{x} \in \mathbb{R}^{N(K+1)}$ if and only if orbit$(\hat{x})$ is a transverse connection, i.e. $\hat{x}$ is a point of transverse intersection of the stable and unstable manifolds. Here non-degenerate means that $DF(\hat{x})$ is an isomorphism. Further, it is shown in [3] that the Newton-like operator T is a contraction about $\bar{x}$ if and only if $DF(\hat{x})$ is an isomorphism. These observations lead to the result that the computer assisted existence proof developed in [3] succedes if and only if the connecting orbit is transverse. Then, for example when applied to homoclinic connectoins, the techniques of [3] prove the existence of chaotic motions via Smale's forcing theorem [4], providing another example of the forcing philosophy outlined in [1].

The remainder of these notes are concerned with certain extensions and amplifications of the discussion above. In particular we discuss the adaptation of these ideas for studying connecting orbits of differential equaiotns. In this reguard there are two important points needing to be addressed.

(I) First: the discussion above pretends that the chart maps P and Q are explicitly know. However in general these maps are only implicitly defined. Then before discussing connecting orbits for differential equations we first review some tools for the numerical study of invariant manifolds in general and stable/unstable manifolds of equilibria and periodic solutions of differential equations in particular. The method we use is called *the Parameterization Method*, and it is based on the notion that the conjugacy relations of dynamical systems theory lead to functional equations describing invariant objects. On the one hand this notion leads to efficient numerical methods for studying invariant manifolds, but on the other hand (the since the invariant manifolds are formulated as the solutions of operator equations) we are also in a natural setting for a-posteriori analysis.

(II) Second: the definition of the connecting orbit operator in Equation (2) above is based on iteration of the map f. Yet when we study differential equations we must apply the flow operator, which is usually only implicitly defined by a vector field. Then also have to discuss some mathematically rigorous techniques for solving initial value problems.

2 The Parameterization Method

The Parameterization Method is a functional analytic framework for studying invariant manifolds for dynamical systems. The method was introduced in a series of papers by de la Llave, Fontich, Cabre, and Haro [5, 6, 7, 8, 9, 10]. The basic idea underpinning the Parameterization Method is simple and is, loosely speaking, based on two observations. First, the notion of equivalence in dynamical systems theory is that of the conjugacy relation. Conjugacy is a notion expressing how one dynamical system embeds another. This embedding can be thought of as an unknown map, in which case the conjugacy becomes an equation for this unknown. The second observation is simply that once a conjugacy if framed as an equation this equation is vulnerable to analysis using all the tools of classical and numerical analysis.

In order to make more than this cartoon explanation we need some definitions and notation. Let X and Y be topological spaces and suppose that $f\colon X \to X$ and $g\colon Y \to Y$ are continuous functions. We say that f is topologically semiconjugate to g if there exists a continuous onto mapping $P\colon Y \to X$ such that

$$f[P(y)] = P[g(y)], \tag{3}$$

for all $y \in Y$. If P is a homeomorphism we say that f and g are topologically conjugate and call P a topological conjugation.

Informally speaking, suppose that $f\colon X \to X$ is a dynamical systems which we are interested in studying, and that $g\colon Y \to Y$ is a simpler dynamical systems whose orbits we understand completely. To say that f is semiconjugate to g says that there is a subsystem of f which has the same dynamics as g. Then semiconjugacy is a tool which is used in dynamical systems theory to embed simple models in complex ones: i.e. to understand when a complicated system has a well understood system as a subsystem. The idea is illustrated in Figure 1.

For example let $f\colon \mathbb{R}^N \to \mathbb{R}^N$ be a diffeomorphism and suppose that $p \in \mathbb{R}^n$ is a fixed point of f. Suppose that the differential $Df(p)$ is hyperbolic, i.e. that none of its eigenvalues are on the unit circle. Then the Hartman-Gorbman theorem says there exists a neighborhood

$$B_r := \left\{x \in \mathbb{R}^N \,|\, \|x\| < r\right\}$$

and a homeomorphism $P\colon B_r \to \mathbb{R}^N$ so that $P(0) = p$ and

$$f[P(y)] = P[Df(p)y],$$

whenever both sides are defined, i.e. for all y such that $Df(p)y \in B_r$. In other words there is a neighborhood of a hyperbolic fixed point p where the dynamics of the full map f are modeled by the dynamics generated by the linear map $Df(p)$.

We are also interested in dynamical systems where time is continuous, i.e. flows. All of the flows considered in the present work will be generated by vector fields. Let $f\colon \mathbb{R}^N \to \mathbb{R}^N$ be an analytic vector field which generates a dynamical system on $\mathbb{R}^N$. Then we let $\phi\colon \mathbb{R}^N \times \mathbb{R} \to \mathbb{R}^N$ denote the flow generated by f, so that

$$\phi(x,0) = x, \qquad \text{for all } x \in \mathbb{R}^N, \tag{4}$$

$$\phi\left(\phi(x,t), s\right) = \phi(x, t+s), \qquad \text{for all } x \in \mathbb{R}^N \quad \text{and } s,t \in \mathbb{R}, \tag{5}$$

and

$$\frac{\partial}{\partial t}\phi(x,t) = f(\phi(x,t)), \tag{6}$$

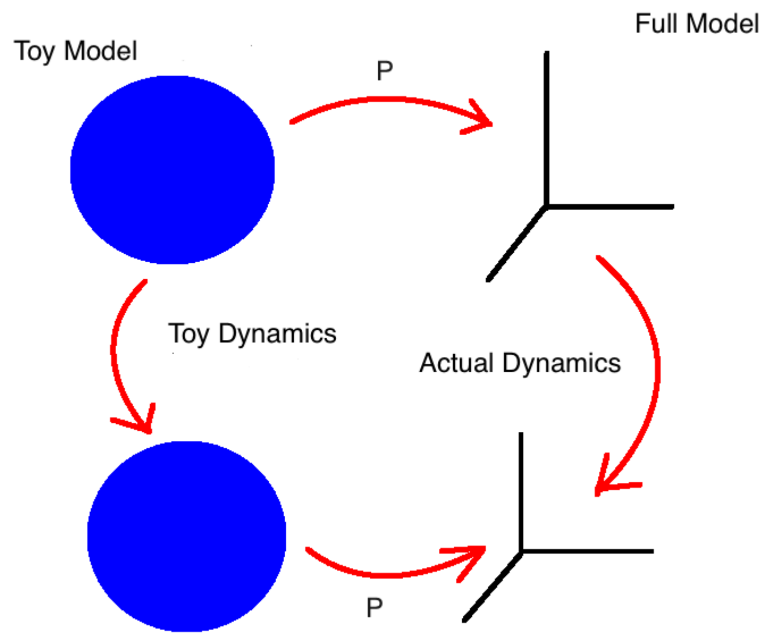

Figure 1: Cartoon of topological conjugacy. The toy model is "embedded" in the real model in a manor preserving the dynamics of the toy. Hence understanding the toy provides partial understanding of the full model.

for all $x \in \mathbb{R}^N$ and $t \in \mathbb{R}$.

Now for $x_0 \in \mathbb{R}^N$ define the orbit of x_0 by

$$\text{orbit}(x_0) = \bigcup_{t \in \mathbb{R}} \phi(x_0, t).$$

Let $p \in \mathbb{R}^n$ be an equilibrium point for f, i.e. suppose that

$$f(p) = 0.$$

Then

$$\phi(p, t) = p,$$

for all $t \in \mathbb{R}$, i.e. p is a fixed point for the flow ϕ. One notion of equivalence for dynamical systems generated by vector fields is as follows.

Theorem 2.1. *Suppose that $f \colon \mathbb{R}^N \to \mathbb{R}^N$, and $g \colon \mathbb{R}^M \to \mathbb{R}^M$ are smooth vector fields with $M \le N$, and that that $P \colon U \subset \mathbb{R}^M \to \mathbb{R}^N$ is a smooth map. If*

$$f[P(s)] = DP(s)g(s), \tag{7}$$

for all $s \in U$ then flow generated by f is semi conjugate on $P[U]$ to the flow generated by g in U. In other words

$$\phi_f(P(s), t) = P[\phi_g(s, t)],$$

for all $s \in U$ and $t > 0$ such that $\phi_g(s, t) \in U$.

Intuitively Equation (7) says that tangent vectors in $\mathbb{R}^m$ are pushed forward under DP to tangent vectors in $\mathbb{R}^N$, i.e. that the vector field f is equal on $P(U)$ to the push forward of the vector field g. The claim follows form existence and uniqueness.

Now, for a given dynamical system f we "guess" or prescribe the desired model dynamics g, and the conjugacy relations (3) and (7) can now be thought of as equations which we hope to solve for the unknown parameterization P. Or, to frame the problem more concretely we define the nonlinear operators $\Psi_{\text{Maps}}, \Psi_{\text{Flows}} \colon \mathcal{X} \to \mathcal{Y}$

$$\Psi_{\text{Maps}}(P)(s) = f[P(s)] - P[g(s)],$$

and

$$\Psi_{\text{Flows}}(P)(s) = f[P(s)] - DP(s)g(s),$$

between appropriate Banach spaces $\mathcal{X}$ and $\mathcal{Y}$, and seek zeros $P \in \mathcal{X}$. This is in essence, the Parameterization Method.

Consider the following examples.

- Fix a vector field $f \colon \mathbb{R}^N \to \mathbb{R}^N$ and take $g \colon \mathbb{R}^N \to \mathbb{R}^N$ the identity function. For $T > 0$ and $x_0 \in \mathbb{R}^N$ let

  $$\mathcal{X} = \left\{ P : P \in C^1([0,T], \mathbb{R}^N) \quad \text{and} \quad P(0) = x_0 \right\},$$

  and $\mathcal{Y} = C^0([0,T], \mathbb{R}^N)$. Then zeros of Ψ_{Flows} correspond to solutions of the initial value problem

  $$f[P(s)] = P'(s), \qquad P(0) = x_0,$$

  on the interval $[0,T]$.

- Similarly, taking f and g as above and P periodic, i.e. $\mathcal{X} = \left\{ P : P \in C^1(\mathcal{S}^1, \mathbb{R}^N) \right\}$ and $\mathcal{Y} = \left\{ Q : Q \in C^0(\mathcal{S}^1, \mathbb{R}^N) \right\}$, we have that zeros of Ψ_{Flows} correspond to limit cycles (periodic orbits) of the vector field f.

- Let $f \colon \mathbb{R}^N \to \mathbb{R}^N$ be a smooth map and let $g \colon \mathbb{S}^1 \to \mathbb{S}^1$ be the rotation map

  $$g(s) = s + \tau \ (\text{mod} 1).$$

  If τ is irrational then the orbit under g of s is dense in $\mathbb{S}^1$ for every s, *i.e.* our model dynamics are given by irrational rotation. Then a zero of Ψ_{Maps} satisfies

  $$f[P(s)] = P(s + \tau),$$

  i.e. the image of P is an invariant circle (as smooth as P). The dynamics on $P(\mathbb{S}^1)$ is conjugate to irrational rotation. In this case the resulting invariant set is a minimal invariant circle. This example generalizes to invariant tori for maps.

- Suppose that $f \colon \mathbb{R}^N \to \mathbb{R}^N$ and $g \colon \mathbb{T}^M \to \mathbb{T}^M$ with $M < N$ are vector fields on Euclidean N space and on the M torus respectively. Consider the case where g is the constant vector field

  $$\begin{aligned} s_1' &= \omega_1 \\ &\vdots \\ s_M' &= \omega_M \end{aligned}$$

with the "frequency vector" $\omega = (\omega_1, \ldots, \omega_M)$ rationally independent. Note that g generates a linear flow on the torus where every orbit is dense. In this case a zero of Φ_{Flow} correspond to a solution of the partial differential equation

$$f[P(\theta)] = \omega_1 \frac{\partial}{\partial s_1} P(s) + \ldots + \omega_M \frac{\partial}{\partial s_M} P(s),$$

and such a solution has

$$\Phi_f(P(s), t) = P(\Phi_g(s, t)),$$

i.e. the flow in the image of P is conjugate to the linear flow on the torus. Then $P(\mathbb{T}^M)$ is an invariant torus for f.

- Define the space

  $$S = \{s = (s_0, s_1, \ldots) : s_k = 0, 1\},$$

  of all infinite sequences of zeros and ones. S is a metric space with metric given by

  $$d(\bar{s}, \hat{s}) = \sum_{n=0}^{\infty} \frac{|\bar{s}_n - \hat{s}_n|}{2^n},$$

  i.e. two sequences are "close" if their entries agree eventually. The "shift map" $g \colon S \to S$ is given by

  $$g(s) = (s_1, s_2, \ldots),$$

  i.e. this map moves every entry of s one space to the left and chops off the first entry. The dynamics generated on S by g a canonical example of "complex dynamics". For example it is an exercise to check that: there are infinitely many periodic orbits, and that they are in fact dense: that there exists a dense orbits, and that the system exhibits so called sensitive dependance on initial conditions (the dynamics of points initially arbitrarily close together are eventually uncorrelated).

  Now let $f \colon \mathbb{R}^N \to \mathbb{R}^N$ be a smooth map. With this set up a zero of Ψ_{Maps} conjugates a subsystem of f to the shift dynamics g. If P is a continuous injection then we say that $P[S]$ is a chaotic subsystem of f.

In later chapters we will use this framework to study conjugacy problems associated with stable/unstable manifolds for some discrete and continuous time dynamical systems. This framework is classical, not in any way due to the author of the present notes. A very nice discussion can be found in the notes of Zhender, but see also the books of Katok and also Robinson (or any standard treatment of dynamical systems theory).

The operators Ψ_{Maps} and Ψ_{Flows} are amenable to the full cannon of analysis's tool: Fixed point and implicit function theorems, perturbation theory, Newton-Kantorovich and Nash-Moser theorems, formal series solution, complex analysis, KAM theory, etcetera. In addition to these classical pen and paper techniques, is fixed specific problems the entire field of numerical analysis is available. In these notes, due to time and space limitations, we focus on using some spectral methods in conjunction with Newton schemes in order to compute numerical approximations of solutions of $\Psi[P] = 0$. However in general collocation methods, finite differencing, finite element, and interpolation methods are all used. The general purpose software package AUTO for example can be used to study numerically a wide variety of problems in dynamical systems theory. In these notes we will usually employ boutique codes written in the MatLab programming language.

Before continuing we mention a few references. Of course for the student of numerical methods for dynamical systems the notes by Carles Simo are a must read [11]. We mention that the work of Lanford, Eckman, Koch, and Wittwer on the Feigenbaum conjectures (work which may have launched the field of computer assisted analysis for dynamical systems theory) is based on the study of a certain conjugacy equation (in this case the Cvitanović renormalization operator) via computer assisted means [12, 13]. We also mention that the seminal work of Warwick Tucker on the computer assisted solution of Smale's 14-th problem (existence of the Lorenz attractor) made critical use of a normal form for the dynamics at the origin of the system. This norm form was computed numerically, and validated numerical bounds obtained by studying a conjugacy equation as referred to above [14, 15].

The original references for the parameterization method, namely [5, 6, 7] for invariant manifolds associated with fixed points, and [8, 9, 10] for invariant manifolds associated with invariant circles, have since launched a small industry. We mention briefly the appearance of KAM theories without action angle variables for area preserving and conformally symplectic systems [16, 17], manifolds associated with invariant tori in Hamiltonian systems [18], phase resetting curves and isochrons [19], quasi-periodic solutions of PDEs [20], and manifolds of mixed-stability [21]. Moreover even more applications are discussed in the references of these papers. We also mention the recent book by Alex Haro, Marta Candell, Jordi-Luis Figueras, and J.M. Mondelo [22].

2.1 Stable/Unstable Manifolds of Equilibria for Differential Equations

2.1.1 The setting and some notation

Consider again a real analytic vector field $f\colon \mathbb{R}^N \to \mathbb{R}^N$ and an equilibrium point $p \in \mathbb{R}^N$, i.e. $f(p) = 0$. We say that p is a hyperbolic equilibrium if $Df(p)$ has no eigenvalues on the imaginary axis. We make the simplifying assumption that $Df(p)$ is diagonalizable, i.e.

$$Df(p) = Q\Sigma Q^{-1},$$

for some diagonal matrix Σ. In fact let

$$\Sigma = \left(\begin{array}{cc} \Sigma_s & 0 \\ 0 & \Sigma_u \end{array} \right),$$

where

$$\Sigma_s = \left(\begin{array}{ccc} \lambda_1^s & \dots & 0 \\ \vdots & \ddots & \\ 0 & \dots & \lambda_{n_s}^s \end{array} \right)$$

is the diagonal matrix of stable eigenvalues and

$$\Sigma_u = \left(\begin{array}{ccc} \lambda_1^u & \dots & 0 \\ \vdots & \ddots & \\ 0 & \dots & \lambda_{n_u}^u \end{array} \right)$$

is the diagonal matrix of unstable eigenvalues. Here

$$\text{real}(\lambda_{n_s}^s) \leq \ldots \leq \text{real}(\lambda_1^s) < 0 < \text{real}(\lambda_1^u) \leq \ldots \leq \text{real}(\lambda_{n_u}^u).$$

The columns of Q are the associated eigenvectors, and we write

$$Q = [\xi_{n_s}^s, \ldots, \xi_1^s, \xi_1^u, \ldots, \xi_{n_u}^u].$$

Let $U \subset \mathbb{R}^N$. The set

$$W^s_{\text{loc}}(p, U) = \{x \in \mathbb{R} \,:\, x \in U \text{ and } \phi(x,t) \in U \text{ for all } t \geq 0\},$$

is called a local stable manifold for p. The stable manifold theorem states that there is an $r > 0$ so that

- The local stable manifold $W^s_{\text{loc}}(p, B_r(p))$ is a smooth, embedded, n_s dimensional disk.
- If $x \in W^s_{\text{loc}}(p, B_r(p))$ is tangent to the stable eigenspace of $Df(p)$ at p.
- If $x \in W^s_{\text{loc}}(p, B_r(p))$ then
$$\lim_{t \to \infty} \phi(x,t) = p.$$

By considering $t \to -\infty$ we obtain the existence of a local unstable manifold $W^u_{\text{loc}}(p, B_r(p))$. As in the case of diffeomorphisms these sets are neither unique nor globally invariant. However by flowing the local sets we obtain the globally invariant manifolds

$$W^s(p) = \bigcup_{t \leq 0} \phi\left(W^s_{\text{loc}}(p, B_r(p)), t\right),$$

and

$$W^u(p) = \bigcup_{t \geq 0} \phi\left(W^u_{\text{loc}}(p, B_r(p)), t\right).$$

2.1.2 Conjugacy and the Invariance Equation

We seek an $r > 0$ and a smooth surjective map $P\colon B_r(0) \subset \mathbb{R}^{n_s} \to \mathbb{R}^N$ so that

$$P[B_r(0)] = W^s_{\text{loc}}(p),$$

i.e. P a chart map for the local unstable manifold. The local stable manifold is approximated to first order by the span of the stable eigenspace, so that

$$P^1(\theta_1, \ldots, \theta_{n_s}) := p + [\xi^s_1, \ldots, \xi^s_{n_s}] \left(\begin{array}{c} \theta_1 \\ \vdots \\ \theta_{n_s} \end{array} \right),$$

is the best linear approximation P.

In order to understand the higher order terms consider the conjugacy relation

$$\phi(P(\theta_1, \ldots, \theta_m), t) = P(e^{\lambda_1 t}\theta_1, \ldots, e^{\lambda_m t}\theta_m), \tag{8}$$

i.e. we ask that P conjugate the flow generated by f to the flow generated by the vector field

$$\theta' = \Lambda_s \theta,$$

where $\theta := (\theta_1, \ldots, \theta_{n_s})^T$. Equation (8) is not terribly useful in practice as it still involves the flow $\phi(x,t)$. In order to obtain a more useful characterization of P we differentiation Equation (8) with respect to time. We obtain

$$\frac{d}{dt}\phi(P(\theta), t) = f(\phi(P(\theta), t)),$$

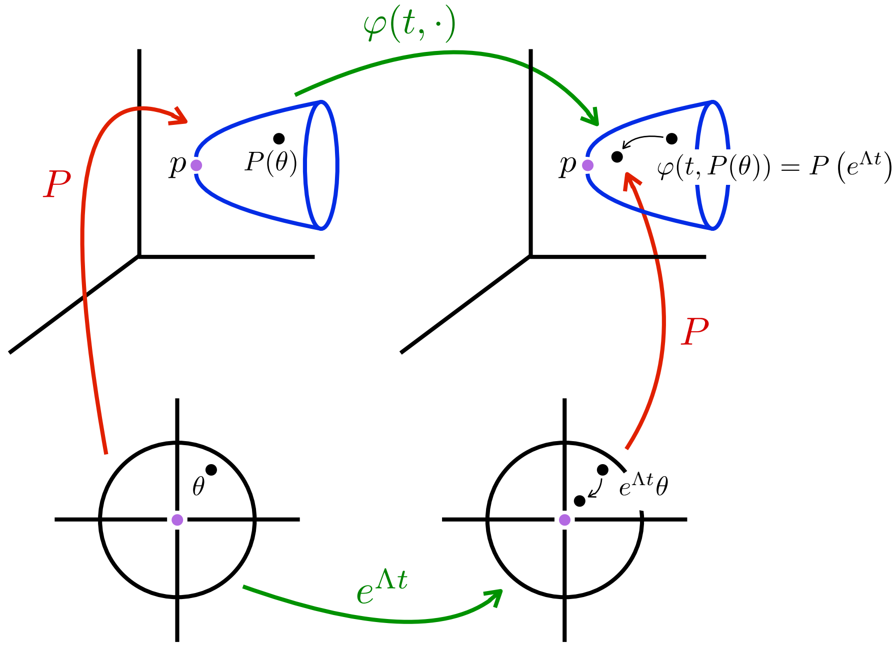

Figure 2: The conjugacy relation at the center of the Parameterization Method for differential equations.

on the left as ϕ is generated by the differential equation $x' = f(x)$. On the right we have

$$\frac{d}{dt}P(e^{\Lambda_s t}\theta) = DP(e^{\Lambda_s t}\theta)\Lambda_s e^{\Lambda_s t}\theta.$$

Taking the limit as $t \to 0$ leads to

$$f(P(\theta)) = DP(\theta)\Lambda_s\theta. \tag{9}$$

We refer to this as the invariance equation for P. The computation above shows that any P solving Equation (8) satisfies the invariance equation (9). The following Lemma shows that the converse holds.

2.1.3 Justification of the Invariance Equation

Lemma 2.2 (Parameterization Lemma)**.** *Let $P\colon D^m \subset \mathbb{R}^m \to \mathbb{R}^n$ be a smooth function with*

$$P(0) = p, \qquad \textit{and} \qquad DP(0) = Q_s. \tag{10}$$

Then $P(\theta)$ satisfies the conjugacy given in Equation (8) if and only if P is a solution of the partial differential equation (9) for all θ in the interior of $D^m(\theta)$.

Proof. Let $P\colon D^m \to \mathbb{R}^n$, be a smooth function with $P(0) = p$ and $DP(0) = Q_s$. Suppose further that $P(\theta)$ solves the partial differential equation (9) in D^m. Choose a fixed $\theta \in D^m$ and fix $t > 0$. Define the function $\gamma\colon [0,t] \to \mathbb{R}^n$ by

$$\gamma(t) \equiv P\left(e^{\Lambda_s t}\theta\right). \tag{11}$$

By using (9) one sees that that γ is the solution of the initial value problem

$$\gamma'(t) = f[\gamma(t)], \qquad \text{and} \qquad \gamma(0) = P(\theta). \tag{12}$$

This means that $\Phi[\gamma(0), t] = \gamma(t)$, hence the conjugacy (**??**) follows from (11) and (12).

Indeed note that $\gamma(0) = P(\theta)$ by definition. Taking the derivative with respect to time of γ for $t > 0$ gives

$$\gamma'(t) = \frac{d}{dt} P\left(e^{\Lambda t}\theta\right) = DP\left(e^{\Lambda t}\theta\right)\Lambda e^{\Lambda t}\theta = f\left[a\left(e^{\Lambda t}\theta\right)\right] = f[\gamma(t)].$$

Here we pass from the first to the second equality by the chain rule, from the second to the third equality by the invariance equation and the fact that $e^{\Lambda t}\theta \in B_\nu^k(0)$ when $t > 0$, and from the third to the forth equation by the definition of γ.

Then $P\left[B_\nu^k(0)\right]$ is forward invariant under the flow, or more precisely $\Phi\left[\gamma(0), t\right] = \gamma(t)$ and the claim that γ solves the desired initial value problem is established. This says that

$$\Phi\left[P(\theta), t\right] = P\left[e^{\Lambda t}\theta\right],$$

(by recalling the definition of the flow map) hence the conjugacy holds.

Suppose on the other hand that P satisfies the conjugacy Equation (8) for all $\theta \in D^m$. Fix $\theta \in D^m$ and differentiate both sides with respect to t in order to obtain

$$f\left(\Phi[P(\theta), t]\right) = DP\left[e^{\Lambda_s t}\theta\right]\Lambda_s e^{\Lambda_s t}\theta.$$

Taking the limit as $t \to 0$ gives that $a(\phi)$ is a solution of Equation (9). This completes the proof. ☐

Remark 2.3. (i) It follows that if $P\colon D^m \to \mathbb{R}^n$ is a smooth function satisfying the linear constraints given by (10) as well as the partial differential equation (9), then the image of P is an immersed forward invariant disk in $W^s(p)$. Moreover P conjugates the dynamics on the range of P to the linear dynamics generated by Λ_s, in the sense of Equation (8). In particular, under the flow Φ the range of P accumulates on p. Hence computing a solution of the PDE subject to the linear constraints gives a means of computing invariant sub-manifolds of $W^s(p)$.

(ii) Conditions providing for the existence of an analytic map $P(\theta)$ satisfying Equation (9) under the constraints given by Equation (10) are developed in [5]. In fact it is necessary and sufficient that no "resonance" of the form

$$\alpha_1\lambda_1 + \ldots + \alpha_k\lambda_k - \lambda_i = 0,$$

occurs, in order that there exists an $a(\phi)$ conjugating the nonlinear flow to the linear flow generated by Λ. Here $\lambda_1, \ldots, \lambda_k \in E_{ss}$, $\lambda_j \in E_s$, and $\alpha = (\alpha_1, \ldots, \alpha_k) \in \mathbb{N}^k$ is any positive multi-index. Since the non-resonance condition relates only stable eigenvalues and positive multi-indices it reduces to a finite number of conditions.

(iii) We remark that the choice of scalings for the eigenvectors in Q_s is free. There are two important points in this regard. First it is shown for example in [5] that the solution equation (9) is unique up to the choice of these scalings. The second (related) point has to do with the Taylor series coefficients of the parameterization map P, and the observation is that the choice of the of eigenvector scalings determines the decay rate of the power series coefficient. In fact this is an obvious corollary of the uniqueness result. The freedom in the choice of the eigenvector scalings is a fact that can be exploited in order to stabilize numerical computations. In particular one often chooses the scalings so that the last coefficient computed has magnitude below some prescribed tolerance. More sophisticated methods are discussed in [23, 24] .

2.1.4 Formal Series Development: example computations

Derivation of the recursion relations which determine the power series coefficients of the chart maps discussed above is best illustrated through some examples. The following computations make plausible the claim that the Parameterization Method can be used to compute manifolds of arbitrary dimension for most of the vector fields encountered in practice.

Example 1 (One dimensional manifold for Lorenz): Consider the Lorenz vector field $f\colon \mathbb{R}^3 \to \mathbb{R}^3$ given by

$$f(x,y,z) = \left(\begin{array}{c} \sigma(y-x) \\ x(\rho - z) - y \\ xy - \beta z \end{array} \right).$$

For $\rho > 1$ the system has three equilibrium points

$$p^0 = \left(\begin{array}{c} 0 \\ 0 \\ 0 \end{array} \right), \qquad \text{and} \qquad p^{1,2} = \left(\begin{array}{c} \pm\sqrt{\beta(\rho-1)} \\ \pm\sqrt{\beta(\rho-1)} \\ \rho - 1 \end{array} \right).$$

Choose one of the three fixed points above and denote it by $\hat{p} \in \mathbb{R}^3$. Let λ denote an eigenvalue of $Df(\hat{p})$, and let ξ denote an associated choice of eigenvector. If λ is a stable eigenvalue then we assume it is the only stable eigenvalue of the fixed point (i.e. the remaining two eigenvalues are unstable). Contrawise if λ is unstable we assume it is the unique unstable eigenvalue (so that the remaining two eigenvalues are stable). We must solve the equation

$$\frac{\partial}{\partial \theta} P(\theta) \lambda \theta = f[P(\theta)].$$

We look for a power series solution of the form

$$P(\theta) = \sum_{n=0}^{\infty} \left(\begin{array}{c} p_n^1 \\ p_n^2 \\ p_n^3 \end{array} \right) \theta^n.$$

Since $P(0) = p$ and P must be tangent to the eigenspace of λ at p we impose the first order conditions

$$p_0 = \hat{p}, \qquad \text{and} \qquad p_1 = \xi.$$

Then

$$\frac{\partial}{\partial \theta} P(\theta) \lambda \theta = \sum_{n=0}^{\infty} n\lambda \left(\begin{array}{c} p_n^1 \\ p_n^2 \\ p_n^3 \end{array} \right) \theta^n,$$

while

$$f(P(\theta)) = \sum_{n=0}^{\infty} \left(\begin{array}{c} \sigma(p_n^2 - p_n^1) \\ \rho\, p_n^1 - p_n^2 - \sum_{k=0}^{n} p_{n-k}^1\, p_k^3 \\ -\beta\, p_n^3 + \sum_{k=0}^{n} p_{n-k}^1\, p_k^2 \end{array} \right) \theta^n.$$

Equating these and matching like powers leads to the equations

$$n\lambda \left(\begin{array}{c} p_n^1 \\ p_n^2 \\ p_n^3 \end{array} \right) = \left(\begin{array}{c} \sigma(p_n^2 - p_n^1) \\ \rho\, p_n^1 - p_n^2 - \sum_{k=0}^{n} p_{n-k}^1\, p_k^3 \\ -\beta\, p_n^3 + \sum_{k=0}^{n} p_{n-k}^1\, p_k^2 \end{array} \right),$$

for all $n \geq 2$. Isolating the terms of order n on the left gives

$$\begin{pmatrix} \sigma(p_n^2 - p_n^1) - n\lambda p_n^1 \\ \rho\, p_n^1 - p_n^2 - p_0^1 p_n^3 - p_0^3 p_n^1 - n\lambda p_n^2 \\ -\beta\, p_n^3 + p_0^1 p_n^2 + p_0^2 p_n^1 - n\lambda p_n^3 \end{pmatrix} = \begin{pmatrix} 0 \\ \sum_{k=1}^{n-1} p_{n-k}^1\, p_k^3 \\ -\sum_{k=1}^{n-1} p_{n-k}^1\, p_k^2 \end{pmatrix},$$

and it is an exercise to show that when expressed in matrix form the above system of equations has the form

$$[Df(p_0) - n\lambda \mathrm{Id}]\, p_n = s_n, \tag{13}$$

where $p_n = (p_n^1, p_n^2, p_n^3)^T$ and

$$s_n := \begin{pmatrix} 0 \\ \sum_{k=1}^{n-1} p_{n-k}^1\, p_k^3 \\ -\sum_{k=1}^{n-1} p_{n-k}^1\, p_k^2 \end{pmatrix}.$$

(To do this exercise one could simply compute the analytic expression for $Df(p_0)$ and checks that it has the form as claimed).

Note that Equation (13) is a linear equation in p_n. Moreover, the right hand side is invertible as long as $n\lambda$ is not an eigenvalue of $Df(p_0)$. But since λ is the only stable eigenvalue we have that $n\lambda < \lambda < 0$ is never an eigenvalue when $n \geq 2$. Then Equation (13) can be solved recursively to compute the Taylor coefficients of P to any desired order. Or phrased another way, the formal series for P is well defined to all orders. We let

$$P^N(\theta) = \sum_{n=0}^{N} p_n \theta^n,$$

denote the N-th order apparoximation.

Example 2: a $2D$ manifold for Lorenz Consider now the case we ignored above, namely let λ_1 and λ_2 be of the same stability (stable or unstable) and assume that the remaining eigenvalue is of the opposite stability (unstable or stable). Then the invariance equation becomes

$$\lambda_1 \theta_1 \frac{\partial}{\partial \theta_1} P(\theta_1, \theta_2) + \lambda_2 \theta_2 \frac{\partial}{\partial \theta_2} P(\theta_1, \theta_2) = f[P(\theta_1, \theta_2)].$$

We seek an analytic parameterization so let

$$P(\theta_1, \theta_2) = \sum_{m=0}^{\infty} \sum_{n=0}^{\infty} \begin{pmatrix} p_{mn}^1 \\ p_{mn}^2 \\ p_{mn}^3 \end{pmatrix} \theta_1^m \theta_2^n.$$

Then a power matching scheme as above leads to the homological equation for $m + n \geq 2$ given by

$$[Df(p_0) - (m\lambda_1 + n\lambda_2)\mathrm{Id}]\, p_{mn} = s_{mn},$$

where

$$s_{mn} = \begin{pmatrix} 0 \\ -\sum_{k=0}^{m} \sum_{l=0}^{n} \delta_{kl}^{mn} p_{(m-k)(n-l)}^1 p_{kl}^3 \\ \sum_{k=0}^{m} \sum_{l=0}^{n} \delta_{kl}^{mn} p_{(m-k)(n-l)}^1 p_{kl}^2 \end{pmatrix}$$

and $\delta_{kl}^{mn} = 0$ if when $k = 0$ and $l = 0$ or when $k = m$ and $l = n$, and is one otherwise (this term makes it easy to express the fact that we have extracted terms of order p_{mn} from the sums).

As above, if $m\lambda_1 + n\lambda_2 \neq \lambda_{1,2}$ then the linear system is uniquely solvable and the formal series for P is well defined to all orders. Then we can recursively solve these homological equations to any desired order in order. Figure 3 shows some parameterized manifolds computed using this method.

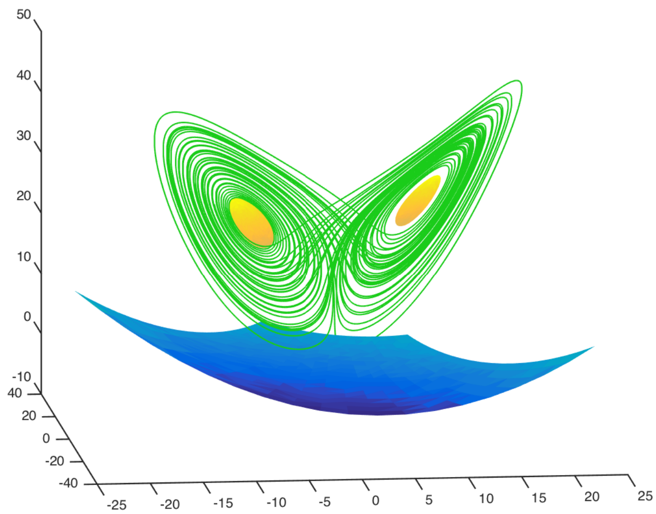

Figure 3: Parameterized Manifolds in the Lorenz system. The orange disks are the two dimensional unstable manifolds of the non-trivial fixed points and the blue is the two dimensional stable manifold of the origin. The green curve depicts a “typical” orbit on the attractor.

Remark 2.4.

- (Complex conjugate eigenvalues) When there are complex conjugate eigenvalues in fact none of the preceding discussion changes. The only modification is that, if we choose complex conjugate eigenvectors, then the coefficients will appear in complex conjugate pairs, i.e.
$$p_{mn} = \overline{p_{mn}}.$$
Then taking the complex conjugate variables gives the parameterization of the real invariant manifold,
$$\hat{P}(\theta_1, \theta_2) := P(\theta_1 + i\theta_2, \theta_1 - i\theta_2),$$
where P is the formal series defined in the preceding discussion. For more details see also [25, 26, 3].

- (Resonance and non-resonance) When the eigenvalues are resonant, i.e. when there is a fixed pair $(\hat{m}, \hat{n}) \in \mathbb{N}^2$ so that
$$\hat{m}\lambda_1 + \hat{n}\lambda_2 = \lambda_j,$$
for either $j = 1$ or $j = 2$, then all is not lost. In this case we cannot conjugate analytically to the diagonalized linear vector field. However by modifying the model vector filed to include a polynomial term which “kills” the resonance the formal computation goes through. The theoretical details are in [5], and numerical implementation with computer assisted error bounds are discussed and implemented in [23].

Exampel 3 (a transcendental vector field by automatic differentiation): Consider the vector field for the pendulum

$$f(x,y) = \left(\begin{array}{c} y \\ -g\sin(x) \end{array} \right).$$

The field has an elliptic equilibrium at $(x,y) = (0,0)$ and a saddle equilibrium at

$$p_0 := \left(\begin{array}{c} \pi \\ 0 \end{array} \right).$$

Let λ be either the stable or unstable eigenvalue of $Df(p_0)$ and let ξ be a choice of associated eigenvector. Let

$$P(\theta) = \sum_{n=0}^{\infty} \left(\begin{array}{c} p_n^1 \\ p_n^2 \end{array} \right) \theta^n,$$

denote the power series for the unknown parameterization. Then the invariance equation becomes

$$\sum_{n=0}^{\infty} n\lambda \left(\begin{array}{c} p_n^1 \\ p_n^2 \end{array} \right) \theta^n = \left(\begin{array}{c} \sum_{n=0}^{\infty} p_n^2 \theta^n \\ -g\sin\left(\sum_{n=0}^{\infty} p_n^1 \theta^n\right) \end{array} \right),$$

and we are left with the task of working out the power series expansion of the sine of an unknown series.

This however can be done via an old trick which appears at least as early as Donald Knuth's *Art of Computer Programming II* [27]. The idea is to introduce the new variables

$$Q(\theta) = \sin(P_2(\theta)),$$

$$R(\theta) = \cos(P_2(\theta))$$

which we can write formally as

$$Q(\theta) = \sum_{n=0}^{\infty} q_n \theta^n,$$

and

$$R(\theta) = \sum_{n=0}^{\infty} r_n \theta^n.$$

Note that

$$q_0 = Q(0) = \sin(p_0^2), \qquad q_1 = Q'(0) = \cos(p_0^2)p_1^2,$$
$$r_0 = R(0) = \cos(p_0^2), \quad \text{and} \quad r_1 = R'(0) = -\sin(p_0^2)p_1^2,$$

are the first order data.

In order to work out the higher order coefficients we note that by the chain rule we have

$$Q'(\theta) = \cos(P_2(\theta))P_2'(\theta) = R(\theta)P_2'(\theta),$$

and

$$R'(\theta) = -\sin(P_2(\theta))P_2'(\theta) = -Q(\theta)P_2'(\theta),$$

or

$$\sum_{n=0}^{\infty}(n+1)q_{n+1}\theta^n = \sum_{n=0}^{\infty}\sum_{k=0}^{n}(k+1)r_{n-k}p_{k+1}^2\theta^n,$$

and

$$\sum_{n=0}^{\infty}(n+1)r_{n+1}\theta^n = -\sum_{n=0}^{\infty}\sum_{k=0}^{n}(k+1)q_{n-k}p^2_{k+1}\theta^n.$$

Matching like powers leads to

$$q_{n+1} = \frac{1}{n+1}\sum_{k=0}^{n}(k+1)r_{n-k}p^2_{k+1},$$

and

$$r_{n+1} = -\frac{1}{n+1}\sum_{k=0}^{n}(k+1)q_{n-k}q^2_{k+1},$$

or

$$q_n = \frac{1}{n}\sum_{k=0}^{n-1}(k+1)r_{n-k-1}p^2_{k+1} = r_0p^2_n + \frac{1}{n}\sum_{k=0}^{n-2}(k+1)r_{n-k-1}p^2_{k+1},$$

and

$$r_n = -\frac{1}{n}\sum_{k=0}^{n-1}(k+1)q_{n-k-1}p^2_{k+1} = -q_0p^2_n - \frac{1}{n}\sum_{k=0}^{n-2}q_{n-k-1}p^2_{k+1},$$

and finally

$$q_n = r_0p^2_n + \frac{1}{n}\sum_{k=1}^{n-1}kr_{n-k}p^2_k,$$

and

$$r_n = -q_0p^2_n - \frac{1}{n}\sum_{k=1}^{n-1}kq_{n-k}p^2_k. \tag{14}$$

Returning to our stable/unstable manifold parameterizations we now have

$$\sum_{n=0}^{\infty}n\lambda\begin{pmatrix} p^1_n \\ p^2_n \end{pmatrix}\theta^n = \sum_{n=0}^{\infty}\begin{pmatrix} p^2_n \\ -gq_n \end{pmatrix}\theta^n.$$

Matching like powers for $n \geq 2$ leads to the equations

$$\begin{aligned} n\lambda p^1_n - p^2_n &= 0 \\ n\lambda p^2_n + gq_n &= 0 \end{aligned}$$

or

$$\begin{aligned} n\lambda p^1_n - p^2_n &= 0 \\ n\lambda p^2_n + gr_0p^2_n &= \frac{-g}{n}\sum_{k=1}^{n-1}kr_{n-k}p^2_k \end{aligned}$$

or finally

$$\begin{pmatrix} n\lambda & -1 \\ 0 & n\lambda + gr_0 \end{pmatrix}\begin{bmatrix} p^1_n \\ p^2_n \end{bmatrix} = \begin{bmatrix} 0 \\ \frac{-g}{n}\sum_{k=1}^{n-1}kr_{n-k}p^2_k \end{bmatrix}.$$

After solving this for $p_n = (p^1_n, p^2_n)^T$ we use Equation (14) to compute r_n going into the next coefficient computation. In this fashion we can computed the taylor expansion parameterization of the stable/unstable manifold for the pendulum to any desired order. Then computing the sine of the unknown power series variable P^1 has the same complexity as computing a Cauchy product of two power series, but the additional cost in memory of storing the coefficients r_n. This technique is these days often referred to as "automatic differentiation" for Taylor series/polynomial manipulation. Again we refer to the book of [22] for a comprehensive treatment. See also the woks [28, 29, 30] for more discussion of automatic differentiation, with and without computer assisted proof, for Taylor series. See also the work of [31] for a version of automatic differentiation for Fourier series.

2.1.5 Validation: the "Taylor Transform"

In Section 4 of [1] in this Lecture series, J.B. van den Berg discusses a functional analytic formulation for computer assisted proof of the existence of periodic orbits for differential equations. Briefly, the steps of the procedure are as follows.

- Project the differential equation onto a Fourier basis via the discrete Fourier transform. This step is aided by the fact that the function space operations of differentiation and multiplication are mapped onto the sequence space operators of multiplication and discrete convolution respectively.

- The transform replaces the problem of finding an unknown function with the problem of solving infinitely many *scalar* equations in infinitely many scalar unknowns. By truncating the infinite system of equations we obtain a system of finitely many nonlinear algebraic equations which can be approximately solved numerically with the aid of the digital computer.

- The truncation errors are quantified by introducing a norm on the space of infinite sequences associated with the unknown Fourier coefficients of the periodic solutions. The topology of the sequence space is dictated by expected Fourier coefficient decay rate, which in For example if the equation is analytic then endowing the solution space with a weighted ℓ^1 norm gives the space a Banach space structure. Now solving the system of scalar equations is equivalent to finding a zero of a given nonlinear map F between Banach spaces.

- Once a choice of topology for the sequence space is made, and an approximate zero of F is found, we proceed to the a-posteriori analysis of the map F. For example the approach based on Theorem 3 combined with the "radii-polynomial" implementation of Section 2.4 discussed in [1] may be used. If successful this a-posteriori analysis allows us to conclude that there is a true zero of F near the approximate zero found using the computer.

- Projecting the sequence solution back into function space gives the quantitative properties of the desired solution of the differential equation.

Nothing prevents the procedure just sketched from being applied to other function space bases and to function space problems other than differential equations. For example in our discussion of stable/unstable manifolds of equilibria for analytic vector fields we developed Formal series expansions of the unknown chart maps via Taylor series. This is appropriate as the unknown function (rather than being periodic as in the examples of [1]) satisfies first order data at a given base point. The unknown Taylor coefficients are now our infinitely many scalar unknowns, and the invariance equation of the Parameterization Method expanded in terms of the unknowns Taylor coefficients provides the scalar equations.

More explicitly, returning briefly to the example of the one dimension manifold of Lorenz, we recast the homological equations in terms of the map

$$F(p^1, p^1, p^3) = \left(\begin{array}{c} F_1(p^1, p^1, p^3) \\ F_2(p^1, p^1, p^3) \\ F_3(p^1, p^1, p^3) \end{array} \right),$$

where $p^1 = \{p_n^1\}_{n=0}^\infty$, $p^2 = \{p_n^2\}_{n=0}^\infty$, and $p^3 = \{p_n^3\}_{n=0}^\infty$ are our infinite sequences of scalar unknowns and the maps $F_{1,2,3}$ have infinitely many scalar components given by

$$F_1(p^1, p^1, p^3)_n = \begin{cases} p_n^1 - q^1 & n = 0 \\ p_n^1 - \xi^1 & n = 1 \\ \sigma(p_n^2 - p_n^2) - n\lambda p_n^1 & n \geq 2 \end{cases}$$

$$F_2(p^1, p^1, p^3)_n = \begin{cases} p_n^2 - q^2 & n = 0 \\ p_n^2 - \xi^2 & n = 1 \\ \rho p_n^1 - p_n^2 - (p^1 * p^3)_n - n\lambda p_n^2 & n \geq 2 \end{cases}$$

and

$$F_3(p^1, p^1, p^3)_n = \begin{cases} p_n^3 - q^3 & n = 0 \\ p_n^3 - \xi^3 & n = 1 \; . \\ \beta p_n^3 + (p^1 * p^2)_n - n\lambda p_n^2 & n \geq 2 \end{cases}$$

Here q denotes the fixed point of Lorenz about which we compute the manifold, (λ, ξ) denotes the chosen stable or unstable eigenvalue/eigenvector pair, and $(a * b)$ denotes the Cauchy product (or discrete-Taylor convolution) of the sequences $\{a_n\}_{n=0}^\infty, \{b_n\}_{n=0}^\infty$, given component wise by

$$(a * b)_n = \sum_{k=0}^{n} a_{n-k} b_k.$$

Now the recursive procedure described in Section 2.1.4 (or a numerical Newton scheme) can be used in order to solve the truncated problem $F(p^1, p^2, p^3) = 0$.

In order to develop a-posteriori analysis for F it is first necessary to topologize our sequence space. By scaling the eigenvectors appropriately (see the uniqueness remark above) we can arrange the our parameterizations are analytic on the unit disk. Then we the classical ℓ^1 norm is appropriate. So, for any $\nu > 0$ and a one sided sequence of complex numbers $a = \{a_n\}_{n=0}^\infty$, we define the norm

$$\|a\|^1 := \sum_{n=0}^{\infty} |a_n| \nu^n.$$

The resulting space

$$\ell^1 := \left\{ a = \{a_n\}_{n=0}^\infty \; : \; \|a\|^1 < \infty \right\},$$

is a Banach space. Moreover the product $*\colon \ell^1 \times \ell^1 \to \ell^1$ induced by the Cauchy product makes ℓ^1 a commutative Banach algebra. (In particular the product $*$ is Fréchet differentiable). It is a classical fact that $(\ell^1)^* = \ell^\infty$, i.e. that the Banach space dual of ℓ^1 is the space

$$\ell^\infty = \left\{ a = \{a_n\}_{n=0}^\infty \; : \; \sup_{n \geq 0} |a_n| < \infty \right\}.$$

This fact is of course useful when studying linear operators on ℓ^1.

Of course if $a \in \ell^1$ then the function

$$f(z) = \sum_{n=0}^{\infty} a_n z^n,$$

is analytic on the unit disk

$$D = \{z \in \mathbb{C} \,:\, |z| < 1\}.$$

Moreover we have the bound

$$\sup_{z \in D} |f(z)| \leq \|a\|^1,$$

by the maximum modulus principle. In other words the ℓ^1 norm of the Taylor coefficients bounds the supremum norm of the function.

With this technology in hand it is possible to develop a-posteriori analysis for the mapping F on the space $\ell^1 \times \ell^1 \times \ell^1$. This analysis enables the computation of mathematically rigorous truncation error bounds for the parameterization of the one dimensional Lorenz manifolds. Moreover, there is nothing about this discussion which is specific to the Lorenz example and in fact an a-posteriori theory for the Parameterization Method can be developed along these lines. The reader interested in the details could consult the recent works [23, 24]. The first of these references encompasses also the treatment of resonant eigenvalues and the second paper deals with automatic algorithms.

2.2 Stable/Unstable Manifolds for Periodic Orbits of Differential Equations

The utility of the Parameterization Method is not limited to the study of invariant manifolds of equilibria. A fairly complete theory for hyperbolic periodic orbits exists, and we describe the broad strokes now. The material in this section is taken from the more complete treatment in [32].

Let $f : \mathbb{R}^d \to \mathbb{R}^d$ be a real analytic vector field and suppose γ is a τ-periodic solution of $\dot{x} = f(x)$ and let $\Gamma = \{\gamma(t) : t \in [0, \tau]\}$ the corresponding periodic orbit. Denote by $\mathbb{T}_{2\tau} = [0, 2\tau]_{/\{0,2\tau\}}$ the circle of length 2τ. Let $\varphi \colon \mathbb{R}^d \times \mathbb{R}^+ \to \mathbb{R}^d$ denote the flow generated by f. We assume without loss of generality that φ is globally well-defined. Suppose that Γ is hyperbolic and consider $\Phi(t) = Q(t)e^{Rt}$ the real Floquet normal form of the fundamental matrix solution of the variational system. Assume that the matrix R is diagonalizable. Let $\lambda_1, \ldots, \lambda_{d_m} \in \mathbb{C}$ denote the stable eigenvalues of the matrix R, that is $\mathrm{Re}(\lambda_i) < 0$ for all $i = 1, \ldots, d_m$, and let $w_1, \ldots, w_{d_m}$ the associated linearly independent eigenvectors. By invertibility of $Q(\theta)$ for all θ, we have that the associated eigenvectors $w_i(\theta) = Q(\theta)w_i$ are linearly independent for all θ. The stable normal bundle of Γ is then parameterized by

$$\mathbb{P}_1(\theta, \sigma) = \gamma(\theta) + \sum_{i=1}^{d_m} w_i(\theta)\sigma_i, \qquad \theta \in \mathbb{T}_{2\tau} \ \text{ and } \ \sigma = (\sigma_1, \ldots, \sigma_{d_m}) \in \mathbb{R}^{d_m},$$

that is $E_s = \mathrm{image}\,(\mathbb{P}_1)$. One goal now is to find a nonlinear correction to $\mathbb{P}_1$ which results in a parameterization of the local stable manifold. In fact we obtain something stronger.

Suppose for the moment that the eigenvalues of R are real and distinct with $\lambda_{d_m} < \ldots < \lambda_1 < 0$. (The case of complex conjugates eigenvalues is similar and the reader interested in the more general ste-up can refer to paper [5]). We consider the vector field

$$\dot{\theta} = 1, \quad \dot{\sigma} = \Lambda \cdot \sigma, \qquad \Lambda \stackrel{\text{def}}{=} \begin{pmatrix} \lambda_1 & & \\ & \ddots & \\ & & \lambda_{d_m} \end{pmatrix}. \tag{15}$$

Let

$$B_\nu \stackrel{\text{def}}{=} \left\{ \sigma \in \mathbb{R}^{d_m} \mid \max_{1 \le i \le d_m} |\sigma_i| \le \nu \right\}.$$

We refer to the cylinder $\mathbb{C}_{2\tau,\nu} \stackrel{\text{def}}{=} \mathbb{T}_{2\tau} \times B_\nu$ as *the parameter space* for the local invariant manifold. Note that the $\sigma = 0$ set is an invariant circle for (15). Also note that the vector field given by (15) is inflowing on the parameter cylinder, that is for any $(\theta, \sigma) \in \partial\, \mathbb{C}_{2\tau,\nu}$ we have that the vector $(1, \Lambda\sigma)$ points inward toward the center of the cylinder. (This is the only place where we exploit that the eigenvalues are real distinct).

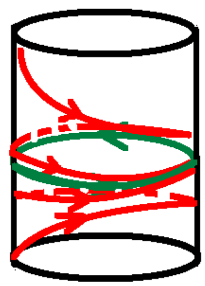

Figure 4: Our toy model of a stable periodic orbit is an attracting orbit on a cylinder. The aim of the Parameterization Methods for the stable manifold of a periodic orbit is to find a covering map conjugating this picture to the full dynamics generated by the vector field f.

We have that the flow on the cylinder is given explicitly by the formula

$$\mathfrak{L}(\theta, \sigma, t) \stackrel{\text{def}}{=} \begin{bmatrix} \theta + t \\ e^{\Lambda t}\sigma \end{bmatrix}, \tag{16}$$

and this flow clearly maps $\mathbb{C}_{2\tau,\nu}$ into its own interior for any $t > 0$, with the circle $\sigma = 0$ a periodic orbit of period 2τ. We take the flow $\mathfrak{L}$ as the "model dynamics" on the stable manifold and look for a chart map which conjugates the nonlinear dynamics on $W^s_{\text{loc}}(\Gamma)$ to the linear dynamics on $\mathbb{C}_{2\tau,\nu}$ given by $\mathfrak{L}$. More precisely we have the following definition.

Definition 2.5 (Conjugating chart map for the local stable manifold). We say that the function $\mathbb{P}\colon \mathbb{T}_{2\tau} \times B_\nu \to \mathbb{R}^d$ is a *conjugating chart map* (or covering map) for a local stable manifold of the periodic orbit Γ if

1. $\mathbb{P}$ is a continuous, injective (one-to-one) mapping of the cylinder $\mathbb{C}_{2\tau,\nu}$ which is real analytic on the interior of the cylinder.

2. $\mathbb{P}(\theta, 0) = \gamma(\theta)$,

3. The conjugacy relation

$$\varphi\left(\mathbb{P}(\theta,\sigma),t\right) = \mathbb{P}\left(\theta + t, e^{\Lambda t}\sigma\right), \tag{17}$$

is satisfied for all $\theta \in \mathbb{T}_{2\tau}$, $\sigma \in B_\nu$, and $t \geq 0$.

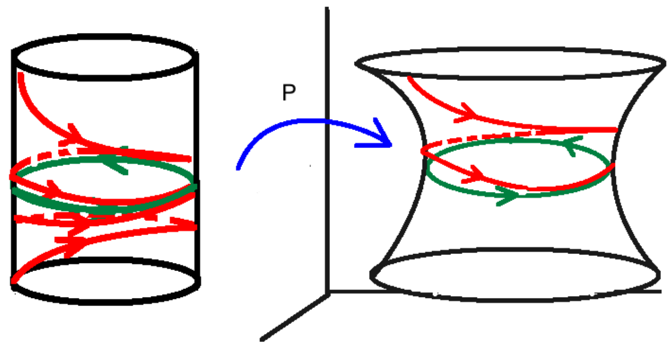

Figure 5: Pictorial illustration of the desired commuting diagram described by Equation (17).

Remark 2.6. Technically we should call $\mathbb{P}$ a covering map for the manifold rather than a chart map, as the model space is a cylinder rather than a Euclidean space. However in the present work we apply the term "chart" liberally and trust that no confusion ensues.

The definition asks that $\mathbb{P}$ conjugates the flow generated by the vector field f to the linear flow generated by (16). If $\mathbb{P}$ is a conjugating chart map then for any $(\theta,\sigma) \in \mathbb{C}_{2\tau,\nu}$,

$$\begin{aligned}
\lim_{t\to\infty} \|\varphi[\mathbb{P}(\theta,\sigma),t] - \gamma(\theta+t)\| &= \lim_{t\to\infty} \left\|\mathbb{P}\left(\theta+t, e^{\Lambda t}\sigma\right) - \gamma(\theta+t)\right\| \\
&= \lim_{t\to\infty} \|\mathbb{P}\left(\theta+t,0\right) - \gamma(\theta+t)\| \\
&= 0
\end{aligned} \tag{18}$$

by continuity of $\mathbb{P}$, the conjugacy relation (17) and the contractiveness of $e^{\Lambda t}$. Hence, the orbit of a point in the image of $\mathbb{P}$ accumulates to the periodic orbit Γ with matching asymptotic phase θ. $\mathbb{P}$ is one-to-one and its image is a d_m dimensional manifold (immersed cylinder). Since image($\mathbb{P}$) is an immersed cylinder containing Γ in its interior and having that each of its points accumulates on Γ under the forward flow, image($\mathbb{P}$) is a local stable manifold for Γ.

The following provides sufficient conditions for the existence of a conjugating chart map.

Theorem 2.7 (**Invariance equation for a conjugating chart map**)**.** *Suppose that* $\mathbb{P}\colon \mathbb{T}_{2\tau} \times B_\nu \to \mathbb{R}^d$ *is a continuous function such that*

$$\mathbb{P}(\theta,0) = \gamma(\theta), \qquad \textit{for all } \theta \in \mathbb{T}_{2\tau}, \tag{19}$$

$\mathbb{P}$ *is differentiable on the circle* $\sigma = 0$ *with*

$$\frac{\partial}{\partial\sigma_i}\mathbb{P}(\theta,0) = w_i(\theta), \qquad \textit{for each } 1 \leq i \leq d_m, \tag{20}$$

and $\mathbb{P}(\theta, \sigma)$ solves the partial differential equation

$$\frac{\partial}{\partial \theta}\mathbb{P}(\theta, \sigma) + \sum_{i=1}^{d_m} \lambda_i \sigma_i \frac{\partial}{\partial \sigma_i}\mathbb{P}(\theta, \sigma) = f(\mathbb{P}(\theta, \sigma)), \tag{21}$$

on the interior of $\mathbb{C}_{2\tau,\nu}$. Then $\mathbb{P}$ is a conjugating chart map for Γ in the sense of Definition 2.5. It follows from (18) that image($\mathbb{P}$) is a local stable manifold for Γ.

Proof. To see that $\mathbb{P}$ is a conjugating chart map choose $(\theta_0, \sigma_0) \in \mathbb{C}_{2\tau,\nu}$, recall (16) and define the curve $x\colon [0, \infty) \to \mathbb{R}^d$ by

$$x(t) = \mathbb{P}(\theta_0 + t, e^{\Lambda t}\sigma_0) = \mathbb{P}(\mathfrak{L}(\theta_0, \sigma_0, t)).$$

Denote $\sigma_0 = (\sigma_1^0, \ldots, \sigma_{d_m}^0) \in B_\nu$. Note that $x(t) \in \text{image}(\mathbb{P})$ for all $t \geq 0$, as $\mathfrak{L}$ is contracting on $\mathbb{C}_{2\tau,\nu}$. Next we show that $x(t)$ solves the initial value problem

$$x'(t) = f(x(t)), \qquad x(0) = \mathbb{P}(\theta_0, \sigma_0), \tag{22}$$

in forward time. To see this note that

$$\begin{aligned} x'(t) &= \frac{d}{dt}\mathbb{P}(\theta_0 + t, e^{\Lambda t}\sigma_0) \\ &= D_{\theta,\sigma}\mathbb{P}(\theta_0 + t, e^{\Lambda t}\sigma_0) \left[\begin{array}{c} 1 \\ e^{\Lambda t}\Lambda \sigma_0 \end{array} \right] \\ &= \frac{\partial}{\partial \theta}\mathbb{P}(\theta_0 + t, e^{\Lambda t}\sigma_0) + \sum_{i=1}^{d_m} \frac{\partial}{\partial \sigma_i}\mathbb{P}(\theta_0 + t, e^{\Lambda t}\sigma_0)\lambda_i e^{\lambda_i t}\sigma_i^0. \end{aligned}$$

Now define the new variables $\hat{\sigma}_i = e^{\lambda_i t}\sigma_i^0$ for $1 \leq i \leq d_m$ and $\hat{\theta} = (\theta_0 + t)_{\text{mod } 2\tau}$. Then for any $t > 0$ we have that $(\hat{\theta}, \hat{\sigma}) \in \text{interior}\,(\mathbb{C}_{2\tau,\nu})$. Since (21) holds on the interior by hypothesis we now have that

$$\begin{aligned} \frac{\partial}{\partial \theta}\mathbb{P}(\theta_0 + t, e^{\Lambda t}\sigma_0) + \sum_{i=1}^{d_m} \frac{\partial}{\partial \sigma_i}\mathbb{P}(\theta_0 + t, e^{\Lambda t}\sigma_0)\lambda_i e^{\lambda_i t}\sigma_i^0 &= \frac{\partial}{\partial \theta}\mathbb{P}(\hat{\theta}, \hat{\sigma}) + \sum_{i=1}^{d_m} \frac{\partial}{\partial \sigma_i}\mathbb{P}(\hat{\theta}, \hat{\sigma})\lambda_i \hat{\sigma}_i \\ &= f\left(\mathbb{P}(\hat{\theta}, \hat{\sigma})\right). \end{aligned}$$

But $\mathbb{P}(\hat{\theta}, \hat{\sigma}) = x(t)$, so this shows that $x'(t) = f(x(t))$ for all $t > 0$ as desired. Since $x(0) = P(\theta_0, \sigma_0)$ by definition we indeed have that $P(\theta_0 + t, e^{\Lambda t}\sigma_0)$ solves (22). But (θ_0, σ_0) was arbitrary in $\mathbb{C}_{2\tau,\nu}$, so this shows that

$$x(t) = \mathbb{P}(\theta + t, e^{\Lambda t}\sigma) = \varphi\left[\mathbb{P}(\theta, \sigma), t\right],$$

and $\mathbb{P}$ satisfies (17) on $\mathbb{C}_{2\tau,\nu}$. Then $\mathbb{P}$ satisfies condition 3 of Definition 2.5. We now establish parts 1 and 2 of Definition 2.5. Since f is real analytic and $\mathbb{P}$ solves the differential equation (21), we have that $\mathbb{P}$ is real analytic in the interior of $\mathbb{C}_{2\tau,\nu}$. From (20) we have that

$$D_\sigma \mathbb{P}(\theta, 0) = [w_1(\theta)| \ldots |w_{d_m}(\theta)].$$

This matrix has full rank because the eigenvectors are linearly independent over $\mathbb{T}_{2\tau}$. Since $\mathbb{P}$ is real analytic it is certainly continuously differentiable, and the continuity of the derivative implies that the differential is full rank in a neighborhood of γ, that is there is an $r > 0$

so that $\|\sigma\| \leq r$ implies that $D_\sigma \mathbb{P}(\theta, \sigma)$ is full rank. If follows from the implicit function theorem that $\mathbb{P}$ is injective for $\|\sigma\| < r$.

Now consider $(\theta_1, \sigma_1), (\theta_2, \sigma_2) \in \mathbb{C}_{2\tau,\nu}$ and suppose that

$$\mathbb{P}(\theta_1, \sigma_1) = \mathbb{P}(\theta_2, \sigma_2). \tag{23}$$

Since $e^{\Lambda t} \to 0$ as $t \to \infty$ there exists $\hat{t} > 0$ such that

$$\left\| e^{\Lambda \hat{t}} \sigma_1 \right\|, \left\| e^{\Lambda \hat{t}} \sigma_2 \right\| < r. \tag{24}$$

Since $\mathbb{P}$ satisfies the conjugacy equation (17) we have that

$$\mathbb{P}\left(\theta_1 + \hat{t}, e^{\Lambda \hat{t}} \sigma_1\right) = \varphi\left(\mathbb{P}(\theta_1, \sigma_1), \hat{t}\right), \qquad \text{and} \qquad \mathbb{P}\left(\theta_2 + \hat{t}, e^{\Lambda \hat{t}} \sigma_2\right) = \varphi\left(\mathbb{P}(\theta_2, \sigma_2), \hat{t}\right).$$

From (23) (as well as the uniqueness of trajectories under φ) it follows that

$$\mathbb{P}\left(\theta_1 + \hat{t}, e^{\Lambda \hat{t}} \sigma_1\right) = \mathbb{P}\left(\theta_2 + \hat{t}, e^{\Lambda \hat{t}} \sigma_2\right).$$

It follows from the conditions of (24) and the fact that $\mathbb{P}$ is injective on $\mathbb{T}_{2\tau} \times B_r$ that

$$\left(\theta_1 + \hat{t}, e^{\Lambda \hat{t}} \sigma_1\right) = \left(\theta_2 + \hat{t}, e^{\Lambda \hat{t}} \sigma_2\right).$$

Since the linear flow map is invertible at $\hat{t}$ we have that $(\theta_1, \sigma_1) = (\theta_2, \sigma_2)$ and $\mathbb{P}$ is an injection of $\mathbb{C}_{2\tau,\nu}$ into $\mathbb{R}^d$. Then $\mathbb{P}$ is a conjugating chart map for the stable manifold of γ as desired. $\square$

We call equation (21) from Theorem 2.7 the *invariance equation.* The preceding discussion shows that in order to study the local invariant manifolds of Γ it is enough to study (21), appropriately constrained. The following provides a necessary condition for the existence of solutions of equation (21), in terms of certain algebraic constraints between the stable eigenvalues.

Definition 2.8 (**Resonant eigenvalues).** We say that the stable eigenvalues $\lambda_1, \ldots, \lambda_{d_m}$ of R are *resonant* at order $\alpha \in \mathbb{N}^{d_m}$ if there is a $1 \leq i \leq d_m$ so that

$$\alpha_1 \lambda_1 + \ldots + \alpha_{d_m} \lambda_{d_m} - \lambda_i = 0. \tag{25}$$

Lemma 2.9 (**Divergence Theorem).** If there is a resonance in the sense of Definition 2.8 at some order $|\alpha| = \alpha_1 + \cdots + \alpha_{d_m} \geq 2$ then the invariance equation (21) has no solution.

So, Lemma 2.9 provides conditions under which we fail to have solutions of the invariance equation (21). But observe that there can be no resonances of order $\alpha \in \mathbb{N}^{d_m}$ when

$$2 \leq |\alpha| \leq \left\lceil \frac{\mathrm{Re}(\lambda_{d_m})}{\mathrm{Re}(\lambda_1)} \right\rceil.$$

That is, if α is large enough then (25) cannot hold as $\mathrm{Re}(\lambda_1), \ldots, \mathrm{Re}(\lambda_{d_m})$ have the same sign. Then in fact there are only a finite number of possible resonances, and this finite number is determined by the "spectral gap" (ratio of the largest and smallest real part taken over the set of stable eigenvalues).

Remark 2.10. *(Resonant Eigenvalues)* Of course resonant eigenvalues do not prevent the existence of the stable manifolds, as can be seen by referring to the stable manifold theorem for a hyperbolic periodic orbit (see for example [33]). Rather a resonance between the eigenvalues is the obstruction to the existence of an analytic conjugacy between the nonlinear flow on the local manifold and the linear dynamics in the eigenspace. When one encounters a resonance the Parameterization Method can still be made to work, but one must conjugate to a polynomial vector field. The polynomial is chosen to "kill" any resonance between the eigenvalues. This is a standard issue in normal form theory. The issues is similar with repeated eigenvalues.

2.2.1 The Homological Equations

In this section we develop a formal series solution for equation (21). Explicitly we assume a series solution of the form

$$\mathbb{P}(\theta, \sigma) = \sum_{|\alpha|=0}^{\infty} a_\alpha(\theta)\sigma^\alpha = \sum_{|\alpha|=0}^{\infty} \sum_{k\in\mathbb{Z}} a_{\alpha,k} e^{\frac{2\pi i}{2\tau}k\theta}\sigma^\alpha. \tag{26}$$

Here $\alpha \in \mathbb{N}^{d_m}$ is a d_m-dimensional multi-index, $a_{\alpha,k} \in \mathbb{R}^d$ for all α, k, $|\alpha| = \alpha_1 + \cdots + \alpha_{d_m}$ and $\sigma^\alpha = \sigma_1^{\alpha_1} \cdots \sigma_{d_m}^{\alpha_{d_m}}$. We refer to expansion (26) as a *Fourier-Taylor series.* We substitute (26) into the invariance equation (21) and expand the vector field $f(\mathbb{P}(\theta, \sigma))$ as its Taylor series with respect to the variable σ evaluated at $\sigma = 0$, that is

$$f(\mathbb{P}(\theta, \sigma)) = f(\mathbb{P}(\theta, 0)) + \sum_{i=1}^{d_m} \frac{\partial}{\partial \sigma_i} f(\mathbb{P}(\theta, 0))\sigma_i + \sum_{|\alpha|\geq 2} \frac{1}{\alpha!} f^{(\alpha)}(\mathbb{P}(\theta, 0))\sigma^\alpha,$$

where $f^{(\alpha)}(\mathbb{P}(\theta, 0))$ is the derivative $\frac{\partial^{|\alpha|}}{\partial \sigma^\alpha} f(\mathbb{P}(\theta, \sigma))$ evaluated at $\sigma = 0$. Then we collect the terms with the same power of σ and we solve the resulting equations. Since

$$\frac{\partial}{\partial \theta}\mathbb{P}(\theta, \sigma) = \sum_{|\alpha|\geq 0} \left(\frac{d}{d\theta} a_\alpha(\theta)\right)\sigma^\alpha, \qquad \frac{\partial}{\partial \sigma_i}\mathbb{P}(\theta, \sigma) = \sum_{|\alpha|>0} a_\alpha \alpha_i \sigma^\alpha \sigma_i^{-1},$$

we end up with the following sequence of differential equations.

$|\alpha| = 0$: The only multi-index with zero length is $\mathbf{0} = (0, \ldots, 0)$. The term in $\sigma^{\mathbf{0}}$ gives

$$\frac{d}{d\theta} a_{\mathbf{0}}(\theta) = f(a_{\mathbf{0}}(\theta))$$

whose solution is given by the periodic orbits itself, hence $a_{\mathbf{0}}(\theta) = \gamma(\theta)$.

$|\alpha| = 1$: The multi-indices of length 1 are $e_i = (0, \ldots, 1, \ldots, 0)$ with 1 in the i-th position. Since $\frac{\partial}{\partial \sigma_i} f(\mathbb{P}(\theta, 0))\sigma_i = Df(a_{\mathbf{0}}(\theta))a_{e_i}(\theta)$, equating the terms in σ^{e_i} for each $i = 1, \ldots, d_m$ yields

$$\begin{cases} \dfrac{d}{d\theta} a_{e_i}(\theta) + \lambda_i a_{e_i}(\theta) = Df(a_{\mathbf{0}}(\theta))a_{e_i}(\theta) \\[2ex] \lambda_i \in \mathbb{R}, \;\; a_{e_i}(\theta) \; 2\tau\text{−periodic.} \end{cases} \tag{27}$$

$|\alpha| \geq 2$: Once $a_{\mathbf{0}}(\theta)$ and $a_{e_i}(\theta)$ are given, we obtain equations of the form

$$\frac{da_\alpha(\theta)}{d\theta} + (\alpha_1\lambda_1 + \ldots + \alpha_{d_m}\lambda_{d_m})a_\alpha(\theta) = Df(a_{\mathbf{0}}(\theta))a_\alpha(\theta) + \boldsymbol{R}_\alpha(\theta), \tag{28}$$

where $\boldsymbol{R}_\alpha$ involves only lower order terms. Equation (28) is referred to as the *homological equation* for the coefficient $a_\alpha(\theta)$ with $|\alpha| \geq 2$. In case the nonlinearities in $f(x)$ are polynomials, the computation of the remaining terms $\boldsymbol{R}_\alpha$ can be done easily by means of the Cauchy products. Indeed the polynomials coincide with the Taylor polynomials.

We now show that all solutions to (27) are given by $(\lambda_i, a_{e_i}(\theta)) = (\lambda_i, Q(\theta)w_i)$ where (λ_i, w_i) is any eigenpair of R. Given a matrix A, denote by $\Sigma(A)$ the set of all (λ, v) such that $Av = \lambda v$.

Proposition 2.11. *Let $\Phi(t) = Q(t)e^{Rt}$ be the real Floquet normal form decomposition of the fundamental matrix solution. Then all the solutions $(\lambda_i, a_{e_i}(\theta))$ of (27) are given by $(\lambda_i, Q(\theta)w_i)$ with $(\lambda_i, w_i) \in \Sigma(R)$.*

Proof. For any λ, the function $\Phi_\lambda(\theta) = \Phi(\theta)e^{-\lambda\theta}$ is the fundamental matrix solution of $\dot{x} = Df(\gamma(t))x - \lambda x$. Indeed

$$\dot{\Phi}_\lambda(\theta) = \dot{\Phi}e^{-\lambda\theta} - \lambda\Phi(\theta)e^{-\lambda\theta} = Df(\gamma(\theta))\Phi(\theta)e^{-\lambda\theta} - \lambda\Phi(\theta)e^{-\lambda\theta} = Df(\gamma(\theta))\Phi_\lambda(\theta) - \lambda\Phi_\lambda(\theta)$$

and $\Phi_\lambda(0) = I$. Let $(\lambda_i, w_i) \in \Sigma(R)$ and let $a_{e_i}(\theta) \stackrel{\text{def}}{=} \Phi_{\lambda_i}(\theta)w_i$. Thus $(\lambda_i, a_{e_i}(\theta))$ is a solution of (27). Moreover, since (λ_i, w_i) is an eigenpair of R, it follows that

$$a_{e_i}(\theta) = \Phi(\theta)e^{-\lambda_i\theta}w_i = e^{-\lambda_i\theta}Q(\theta)e^{R\theta}w_i = e^{-\lambda_i\theta}Q(\theta)e^{\lambda_i\theta}w_i = Q(\theta)w_i$$

proving that $a_{e_i}(\theta)$ is 2τ-periodic. We conclude that $(\lambda_i, Q(\theta)w_i)$ is a solution of (27).

On the contrary, suppose $(\lambda_i, a_{e_i}(\theta))$ is a solution of problem (27). Thus

$$a_{e_i}(\theta) = \Phi_{\lambda_i}(\theta)a_{e_i}(0) = \Phi(\theta)e^{-\lambda_i\theta}a_{e_i}(0).$$

Since $a_{e_i}(\theta)$ is 2τ-periodic, $a_{e_i}(0) = a_{e_i}(2\tau) = \Phi(2\tau)e^{-\lambda_i 2\tau}a_{e_i}(0)$, that is $(e^{2\lambda_i\tau}, a_{e_i}(0)) \in \Sigma(\Phi(2\tau))$. From the real Floquet normal form decomposition, we have that $\Phi(2\tau) = Q(2\tau)e^{2\tau R} = e^{2\tau R}$. Moreover, the spectrum of R is in one-to-one correspondence with the spectrum of $\Phi(2\tau)$ since $(\lambda, w) \in \Sigma(R)$ if and only if $(e^{2\tau\lambda}, w) \in \Sigma(\Phi(2\tau))$. We conclude that $a_{e_i}(0) = w_i$ and $(\lambda_i, w_i) \in \Sigma(R)$. From this it follows that $a_{e_i}(\theta) = Q(\theta)w_i$. $\square$

The existence of 2τ-periodic solutions of (28) is discussed in the following result whose proof can be found in [7].

Theorem 2.12. *If $e^{2\nu\tau}$ is not an eigenvalue of $\Phi(2\tau)$ then, for any 2τ-periodic function $\boldsymbol{R}_\alpha$, there exists a 2τ-periodic solution a_α of $(\frac{d}{d\theta} - Df(a_{\mathbf{0}}) + \nu)a_\alpha = \boldsymbol{R}_\alpha$.*

Taking $\nu = \alpha_1\lambda_1 + \ldots + \alpha_{d_m}\lambda_{d_m}$, if $e^{2(\alpha_1\lambda_1+\ldots+\alpha_{d_m}\lambda_{d_m})\tau}$ is not an eigenvalue of $\Phi(2\tau)$, there exist 2τ-periodic functions $a_\alpha(\theta)$ solutions of (28). That comes from the previous theorem and from the fact that the remaining term $\boldsymbol{R}_\alpha$ is 2τ-periodic.

2.2.2 Efficient Solution of the Homological Equations Using the Floquet Normal Form

The situation just encountered, namely where one is trying to solve an invariance equation for a conjugating map and finds that the problem reduces to solving infinitely many linear equations, is not uncommon. It arises frequently in the study of normal forms. As often happens in normal form theory we find that solving the resulting system of infinitely many linear differential equations is nontrivial, and seek further reduction.

Recall that the Floquet normal form Q is a solution of the differential equation

$$Q'(\theta) + Q(\theta)R = Df(\gamma(\theta))Q(\theta) \tag{29}$$

with R a real-valued matrix. We assume that R is diagonalizable, that is that there exists M such that

$$R = M\Sigma M^{-1},$$

with

$$\Sigma = \begin{pmatrix} \Lambda_s & 0 & 0 \\ 0 & \Lambda_u & 0 \\ 0 & 0 & 0 \end{pmatrix}.$$

Here Λ_s is the $d_m \times d_m$ diagonal matrix of eigenvalues with negative real parts and Λ_u is the diagonal matrix of eigenvalues with positive real parts. As before $w_1, \ldots, w_{d_m}$ are the linearly independent eigenvectors associated with the stable eigenvalues. Again the functions $w_j(\theta) = Q(\theta)w_j$ parameterize the stable invariant normal bundle.

We will now see that the homological equation (28) is reduced to constant coefficient by the Floquet normal form. For $|\alpha| \geq 2$ define the functions $w_\alpha(\theta) : \mathbb{T}_{2\tau} \to \mathbb{R}^d$ by the coordinate transformation

$$a_\alpha(\theta) = Q(\theta)w_\alpha(\theta).$$

Taking into account (29), the homological equation (28) is transformed into the constant coefficient ordinary differential equation

$$\frac{d}{d\theta} w_\alpha(\theta) + \left((\alpha_1\lambda_1 + \ldots + \alpha_{d_m}\lambda_{d_m})I - R\right) w_\alpha(\theta) = Q^{-1}(\theta)\boldsymbol{R}_\alpha(\theta). \tag{30}$$

We now expand w_α as

$$w_\alpha(\theta) = \sum_{k\in\mathbb{Z}} w_{\alpha,k} e^{\frac{2\pi i k}{2\tau}\theta}, \qquad (w_{\alpha,k} \in \mathbb{C}^d)$$

and

$$Q^{-1}(\theta)\boldsymbol{R}_\alpha(\theta) = \sum_{k\in\mathbb{Z}} A_{\alpha,k} e^{\frac{2\pi i k}{2\tau}\theta}, \qquad (A_{\alpha,k} \in \mathbb{C}^d).$$

We make a final coordinate transformation and define $v_{\alpha,k}$ by

$$w_{\alpha,k} = M v_{\alpha,k}.$$

Then equation (30) gives

$$v_{\alpha,k} = \left[\left(\frac{2\pi i k}{2\tau} + \alpha_1\lambda_1 + \ \ldots + \alpha_{d_m}\lambda_{d_m}\right) I - \Sigma\right]^{-1} M^{-1}A_{\alpha,k}.$$

But this is diagonalized and solving component-wise we obtain

$$v_{\alpha,k}^{(j)} = \frac{1}{\frac{2\pi i k}{2\tau} + \alpha_1\lambda_1 + \ldots + \alpha_{d_m}\lambda_{d_m} - \lambda_j} (M^{-1}A_{\alpha,k})^{(j)}, \tag{31}$$

for $1 \leq j \leq d_m$. Working backward from $v_\alpha(\theta)$ we obtain the desired solution $a_\alpha(\theta)$ by

$$a_\alpha(\theta) = Q(\theta)M v_\alpha(\theta). \tag{32}$$

Remark 2.13 (**Resonances revisited).** The Fourier-Taylor coefficients $v_{\alpha,k}^{(j)}$ defined by (31) are formally well defined to all orders precisely when there are no resonances in the sense of Definition 2.8. This fact establishes Lemma 2.9.

Remark 2.14 (Efficient numerical computations). If the Fourier coefficients for both the periodic solution $\gamma(\theta)$ and $Q(\theta)$ are known, then the recurrence equations given in (31) combined with the coordinate transformation given by (32) provide a recipe for computing the conjugating chart map $\mathbb{P}(\theta, \sigma)$ to any desired finite order.

Remark 2.15 (The case of complex conjugates eigenvalues of $\boldsymbol{R}$). Assume that $\lambda_{1,2} = a \pm ib$ are eigenvalues of the matrix R coming from the Floquet normal. For sake of simplicity of the presentation, assume that $d_m = 2$. In this case we still conjugate to the flow given by (17), however we do not obtain real results when we flow by

$$e^{\Lambda t}\sigma = \exp\left(\begin{bmatrix} a+ib & 0 \\ 0 & a-ib \end{bmatrix} t\right)\begin{bmatrix} \sigma_1 \\ \sigma_2 \end{bmatrix}.$$

Because of this the coefficients of the parameterization $\mathbb{P}$ will not be real either. Note however that the linear flow still takes complex conjugate arguments to complex conjugate results. This property is then inherited by the parameterization coefficients and is then exploited to obtain a real result. Making the usual complex conjugate variables $\sigma_1 = t + is$ and $\sigma_2 = t - is$ we observe, by considering the recurrence equations (31), that the coefficients a_{α_1,α_2} for the parameterization have that property that $a_{\alpha_1,\alpha_2}(\theta) = \overline{a_{\alpha_2,\alpha_1}(\theta)}$. Then, as long as we have chosen complex conjugate eigenvectors, the complex conjugate change of variables are precisely what is needed in order to obtain a real valued function, that is

$$\mathbb{P}(\theta, s+it, s-it) \in \mathbb{R}^d$$

for all θ, s, t. This is the same idea used in [25, 34, 26] in order to parameterize real invariant manifolds associated with fixed points when there are complex conjugate eigenvalues. See the works just cited for more thorough discussion. The case $d_m > 2$ is similar.

Remark 2.16 (The parameterization and non-orientability of the manifold). Note that even if the stable/unstable manifold is non-orientable, the τ-periodic orbit Γ is a τ-periodic geometrical object. Then the 2τ-periodic parametrization $\mathbb{P}(\theta, \sigma)$ should cover twice the same manifold. In general, we then have two possibilities:

$$\mathbb{P}(\theta+\tau, \sigma) = \mathbb{P}(\theta, \sigma) \qquad \text{or} \qquad \mathbb{P}(\theta+\tau, \sigma) = \mathbb{P}(\theta, -\sigma).$$

The first possibility is when $Q(t)$ is τ-periodic in which case the normal bundle is orientable. If the normal bundle is non-orientable, then we are in the second case. More precisely, the relation $\mathbb{P}(\theta+\tau, \sigma) = \mathbb{P}(\theta, -\sigma)$ implies that

$$\sum_{n\geq 0} a_n(\theta+\tau)\sigma^n = \sum_{n\geq 0} a_n(\theta)(-\sigma)^n.$$

Therefore, $a_n(\theta+\tau) = a_n(\theta)$ for n even and $a_n(\theta+\tau) = -a_n(\theta)$ for n odd, that is a_n is τ-periodic for n even and a_n is 2τ-periodic but odd in $\theta = \tau$ for odd n, a relation that $a^0 = \gamma$ and a^1 satisfy. In practice our computations result in a sequence of a_n with exactly the above properties. Thus we can restrict to positive σ and $\theta \in [0, 2\tau]$ or $\sigma \in [-\delta, \delta]$ and $\theta \in [0, \tau]$ in order to parameterize the complete manifold.

2.2.3 Examples: Lorenz, Arneodo, Rössler, and truncated Kuramoto-Sivashinsky systems

Lorenz: The full computation of the homological equations, including the derivation of the precise form of the right-hand-sides $\boldsymbol{R}_\alpha(\theta)$ is best illustrated in the context of specific examples. To this end, recall that the Lorenz equations are given by the quadratic vector field

$$f(x,y,z) = \begin{pmatrix} -sx+sy \\ \rho x - y - xz \\ -\beta z + xy \end{pmatrix}, \qquad (s,\beta,\rho \in \mathbb{R}). \tag{33}$$

We expand the τ-periodic solution γ by considering it as a 2τ-periodic function, and consider the Fourier expansion of the 2τ-periodic matrix Q, that is

$$\gamma(\theta) = \sum_{k\in\mathbb{Z}} \gamma_k e^{\frac{2\pi i k}{2\tau}\theta} \qquad \text{and} \qquad Q(\theta) = \sum_{k\in\mathbb{Z}} Q_k e^{\frac{2\pi i k}{2\tau}\theta}.$$

Choose $(\lambda, w) \in \Sigma(R)$, $\lambda \neq 0$. In this section, we only consider orbits with one dimensional stable and unstable manifolds. Hence, for each manifold, we seek a function of the form

$$\mathbb{P}(\theta,\sigma) = \sum_{\alpha=0}^{\infty} a_\alpha(\theta)\sigma^\alpha = \sum_{\alpha=0}^{\infty}\sum_{k\in\mathbb{Z}} a_{\alpha,k} e^{\frac{2\pi i k}{2\tau}\theta}\sigma^n. \tag{34}$$

Denote $a_\alpha = (a_\alpha^{(1)}, a_\alpha^{(2)}, a_\alpha^{(3)})^T \in \mathbb{R}^3$ and $\mathbb{P} = (\mathbb{P}_1, \mathbb{P}_2, \mathbb{P}_3)^T$. Then we require that $\mathbb{P}(\theta,0) = \gamma(\theta)$ and $\frac{\partial}{\partial\theta}\mathbb{P}(\theta,0) = w(\theta)$ and take the Fourier-Taylor coefficients (of Taylor order 0 and 1) to be

$$a_{0,k} = \gamma_k \qquad \text{and} \qquad a_{1,k} = Q_k w,$$

for all $k \in \mathbb{Z}$. This determines the parameterization to first order. In order to determine the higher order coefficients we plug the unknown expansion given by (34) into the invariance equation (21) and obtain

$$\frac{\partial}{\partial\theta}\mathbb{P}(\theta,\sigma) + \lambda\sigma\frac{\partial}{\partial\sigma}\mathbb{P}(\theta,\sigma) = \begin{pmatrix} -s\mathbb{P}_1(\theta,\sigma) + s\mathbb{P}_2(\theta,\sigma) \\ \rho\mathbb{P}_1(\theta,\sigma) - \mathbb{P}_2(\theta,\sigma) - (\mathbb{P}_1\cdot\mathbb{P}_3)(\theta,\sigma) \\ -\beta\mathbb{P}_3(\theta,\sigma) + (\mathbb{P}_1\cdot\mathbb{P}_2)(\theta,\sigma) \end{pmatrix}, \tag{35}$$

where

$$(\mathbb{P}_1\cdot\mathbb{P}_2)(\theta,\sigma) = \sum_{\alpha=0}^{\infty} p_\alpha^{(1,2)}(\theta)\sigma^\alpha \quad \text{and} \quad (\mathbb{P}_1\cdot\mathbb{P}_3)(\theta,\sigma) = \sum_{\alpha=0}^{\infty} p_\alpha^{(1,3)}(\theta)\sigma^\alpha,$$

with

$$p_\alpha^{(1,2)}(\theta) \stackrel{\text{def}}{=} \sum_{\substack{\alpha_1+\alpha_2=\alpha \\ \alpha_i\geq 0}}^{\infty} a_{\alpha_1}^{(1)}(\theta)a_{\alpha_2}^{(2)}(\theta) \quad \text{and} \quad p_\alpha^{(1,3)}(\theta) \stackrel{\text{def}}{=} \sum_{\substack{\alpha_1+\alpha_2=\alpha \\ \alpha_i\geq 0}}^{\infty} a_{\alpha_1}^{(1)}(\theta)a_{\alpha_2}^{(3)}(\theta).$$

It is convenient to separate in $p_\alpha^{(i,j)}$ the highest order terms in α, that is

$$\begin{aligned} p_\alpha^{(1,2)}(\theta) &= a_\alpha^{(1)}(\theta)a_0^{(2)}(\theta) + a_0^{(1)}(\theta)a_\alpha^{(2)}(\theta) + \tilde{p}_\alpha^{(1,2)}(\theta) \\ p_\alpha^{(1,3)}(\theta) &= a_\alpha^{(1)}(\theta)a_0^{(3)}(\theta) + a_0^{(1)}(\theta)a_\alpha^{(3)}(\theta) + \tilde{p}_\alpha^{(1,3)}(\theta), \end{aligned}$$

with

$$\tilde{p}_\alpha^{(1,2)}(\theta) \stackrel{\text{def}}{=} \sum_{\substack{\alpha_1+\alpha_2=\alpha \\ \alpha_i> 0}}^{\infty} a_{\alpha_1}^{(1)}(\theta)a_{\alpha_2}^{(2)}(\theta) \quad \text{and} \quad \tilde{p}_\alpha^{(1,3)}(\theta) \stackrel{\text{def}}{=} \sum_{\substack{\alpha_1+\alpha_2=\alpha \\ \alpha_i> 0}}^{\infty} a_{\alpha_1}^{(1)}(\theta)a_{\alpha_2}^{(3)}(\theta).$$

The reason of the last definition stands on the fact that, when matching like powers of σ in the right term of (35), the coefficient of σ^α is given by

$$\begin{pmatrix} -sa_\alpha^{(1)} + sa_\alpha^{(2)} \\ \rho a_\alpha^{(1)} - a_\alpha^{(2)} - p_\alpha^{(1,3)} \\ -\beta a_\alpha^{(3)} + p_\alpha^{(1,2)} \end{pmatrix} = Df(a_0)a_\alpha + \boldsymbol{R}_\alpha(\theta) \stackrel{\text{def}}{=} Df(a_0)a_\alpha + \begin{pmatrix} 0 \\ -\tilde{p}_\alpha^{(1,3)}(\theta) \\ \tilde{p}_\alpha^{(1,2)}(\theta) \end{pmatrix},$$

where the function $\boldsymbol{R}_\alpha(\theta)$ involves only lower order terms. Therefore, matching the coefficients of σ^α in (35), it follows that the functions $a_\alpha(\theta)$ satisfy the differential equations

$$\frac{d}{d\theta}a_\alpha(\theta) + \lambda\alpha a_\alpha(\theta) - Df(\gamma(\theta))a_\alpha(\theta) = \boldsymbol{R}_\alpha(\theta). \tag{36}$$

Here we have used the fact that $a_0(\theta) = \gamma(\theta)$ as well as the analytic expression for $Df(x, y, z)$. Equation (36) is referred to as the *homological equation* for the coefficients of $\mathbb{P}$. Now that $\boldsymbol{R}_\alpha(\theta)$ is known, the parameterization coefficients are computed directly using (31).

Remark 2.17 (Non-resonance and numerics for Lorenz).
• In the present situation the denominator in (31) is one of the following

$$\frac{2\pi ik}{2\tau} + \alpha\lambda - \lambda_s, \qquad \frac{2\pi ik}{2\tau} + \alpha\lambda - \lambda_u, \qquad \text{or} \qquad \frac{2\pi ik}{2\tau} + \alpha\lambda,$$

and none of these are ever zero, due to the assumption that Γ is hyperbolic (one stable and one unstable eigenvalue) as well as the condition that $\alpha \geq 2$. Then the solution given by (31) is formally well-defined to all orders. In fact this is always true of a two dimensional stable/unstable manifold of a periodic orbit associated with a single eigendirection: there can be no resonances in this case. This was already shown in [7] without the use of the Floquet theory and exploited for numerical purposes in [35, 19].
• While (31) gives an explicit representation of the components of the k-th Fourier coefficient of the α-th solution function $v_\alpha(\theta)$ for all k and α, the coefficients $A_{\alpha,k}$ are convolution coefficients depending on the coefficients of $\boldsymbol{R}_\alpha$ and Q^{-1}. Then in fact

$$A_{\alpha,k} = \sum_{\ell\in\mathbb{Z}} (\boldsymbol{R}_\alpha)_{k-\ell}(Q^{-1})_\ell,$$

and the coefficients of $\boldsymbol{R}_\alpha$ are themselves convolutions involving lower order terms of $\mathbb{P}$. Since we are dealing with Fourier series all of the convolution sums are infinite series. However in practice we only compute finitely many Fourier coefficients for γ, Q and hence for $\boldsymbol{R}_\alpha$. For example in the Lorenz computations discussed above we have for $\alpha = 2$

$$\boldsymbol{R}_2(\theta) = \begin{pmatrix} 0 \\ -a_1^{(1)}(\theta)a_1^{(3)}(\theta) \\ a_1^{(1)}(\theta)a_1^{(2)}(\theta) \end{pmatrix} = \begin{pmatrix} 0 \\ -w^{(1)}(\theta)w^{(3)}(\theta) \\ w^{(1)}(\theta)w^{(2)}(\theta) \end{pmatrix}.$$

But $w(\theta) = Q(\theta)w = \left(w^{(1)}(\theta), w^{(2)}(\theta), w^{(3)}(\theta)\right)$ is only known numerically up to K modes, hence $\boldsymbol{R}_2(\theta)$ is only computed approximately. Similar comments apply for all $\alpha \geq 2$, so that all $A_{\alpha,k}$ are only known up to a finite number of terms and we only know the functions $v_\alpha(\theta)$ approximately. This makes a-posteriori analysis especially valuable when assessing the quality of the resulting approximation. However small defect does not imply good approximation, and ultimately one would like to have a method for validating the error associated with the approximation in a mathematically rigorous way.

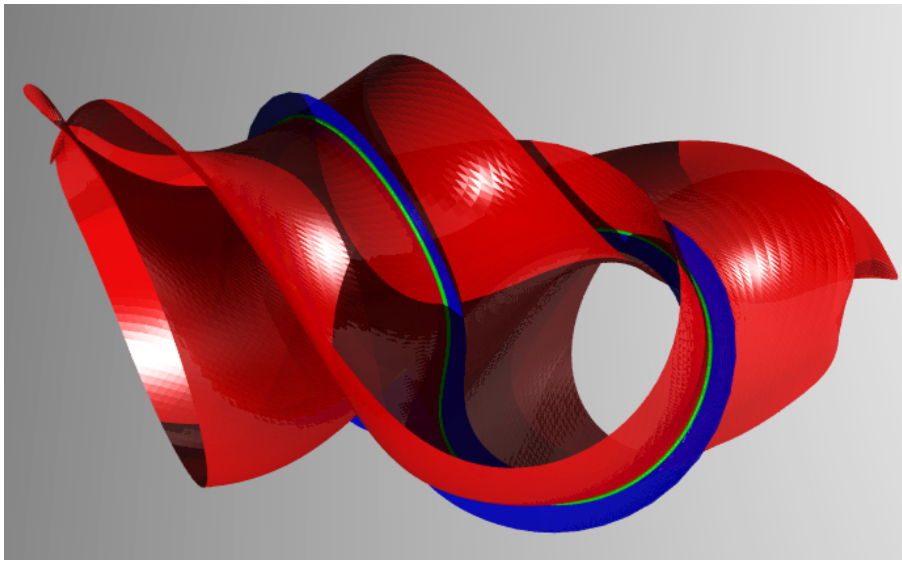

Figure 6: Local stable (red) and unstable (blue) manifolds associated with a hyperbolic periodic orbit Γ (green) in the Lorenz attractor. This computation illustrated here is carried out for the classical parameter values $\rho = 28$, $s = 10$ and $\beta = 8/3$. The Figure illustrates the images of the stable and unstable parameterizations truncated to Taylor order $N = 25$ and $K = 66$ Fourier modes. No numerical integration has been performed in order to extend the local the manifolds. Note that the stable manifold is not the graph of a function over the stable linear bundle of Γ. This highlights an important feature of the Parameterization Method which is that it can follow folds in the manifolds. The Figure also illustrates the stretching and folding of the phase space near Γ.

• In light of the previous remarks we must ask: is the scheme described here at all reasonable? The answer will depend ultimately on the regularity of the vector field f. If f is analytic then γ, Q, and ultimately $\mathbb{P}$ are analytic functions and hence have Fourier-Taylor coefficients which decay exponentially. In this case it is reasonable to expect that some finite number of modes represent the function very well, and that in each convolution term the contributions of higher order modes is not very important. If in a particular example f is less regular, or if the Fourier-Taylor coefficients decay too slowly, then this may not be the case and the procedure proposed in the present work may fail.
• To this point we have said nothing about the scaling of the eigenvectors. It is worth mentioning that the freedom of choice in this scaling can be used in order to control the decay rate of the Taylor coefficients in the expansion. This provides a "knob" which can be used in order to control the numerical stability of expansion. The trade off is that for a fixed choice of ν decreasing the scale of the eigenvector decreases the size of the image of the parameterization in phase space.

Arneodo: Consider the Arneodo system (with $\beta = 2$ and $\alpha = 3.372$)

$$\begin{cases} \dot{x} = y \\ \dot{y} = z \\ \dot{z} = \alpha x - x^2 - \beta y - z, \end{cases} \tag{37}$$

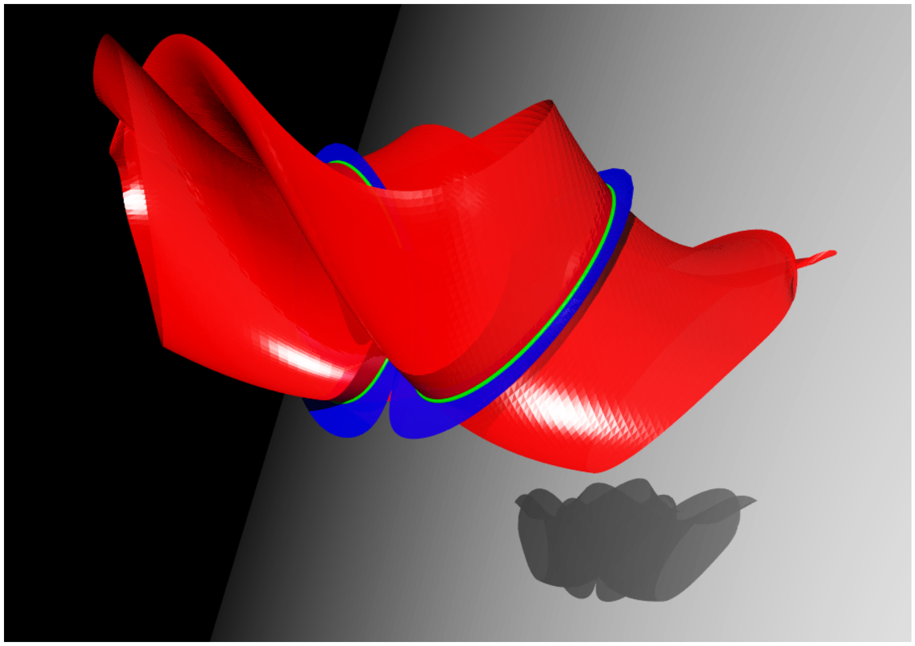

Figure 7: Local stable (red) and unstable (blue) manifolds of a hyperbolic periodic orbit Γ (green) in the Lorenz attractor at the classical values $\rho = 28$, $s = 10$ and $\beta = 8/3$. This Figure illustrates that the Parameterization Method provides approximations for local invariant manifolds which are valid in a large region about Γ, and which expose nonlinear features of the manifolds. Moreover "valid" may be quantified by measuring the defect associated with the truncated expansion (for numerical results regarding this example see Tables 1 and 2).

It admits a periodic orbit Γ with period roughly $\tau = 4.5328$. The complex matrix B in the complex Floquet normal form has the following eigenvalues

$$\mu_1 = -1.0935 + 0.6931i, \qquad \mu_2 = 0.0935 + 0.6931i, \qquad \mu_3 = 0.$$

Since $\mathrm{Re}(\mu_1) < 0$ and $\mathrm{Re}(\mu_2) > 0$, $\dim(W^s(\Gamma)) = \dim(W^u(\Gamma)) = 1$. Two eigenvalues of B are of the form $\mu = \nu + \frac{i\pi}{\tau} \in \mathbb{C}$. Each Floquet exponent corresponds to the Floquet multiplier $\phi_i = e^{\mu_i \tau}$, that is $\phi_1 = -0.0070$ and $\phi_2 = -1.5275$, which are both real negative. Hence, the orientation of the eigenvector $w_i(\theta) = Q(\theta) w_i$ is flipped over $[0, \tau]$ and the corresponding linear bundles are Mobius strips.

Rössler: We now compute a three dimensional stable manifold in the Rössler system

$$\left\{ \begin{array}{l} \dot{x} = -(y + z) \\ \dot{y} = x + \frac{1}{5} y \\ \dot{z} = \frac{1}{5} + z(x - \lambda). \end{array} \right. \tag{38}$$

For small λ the system has a single fully attracting periodic orbit. As λ increases the periodic orbit undergoes a period doubling cascade giving rise to a chaotic attractor. We set $\lambda = 0.5$ and compute the periodic orbit and Floquet normal form using $K = 45$ Fourier modes. The period of the orbit is roughly $\tau = 5.0832$, the eigenvalues of B are real (and therefore coincide

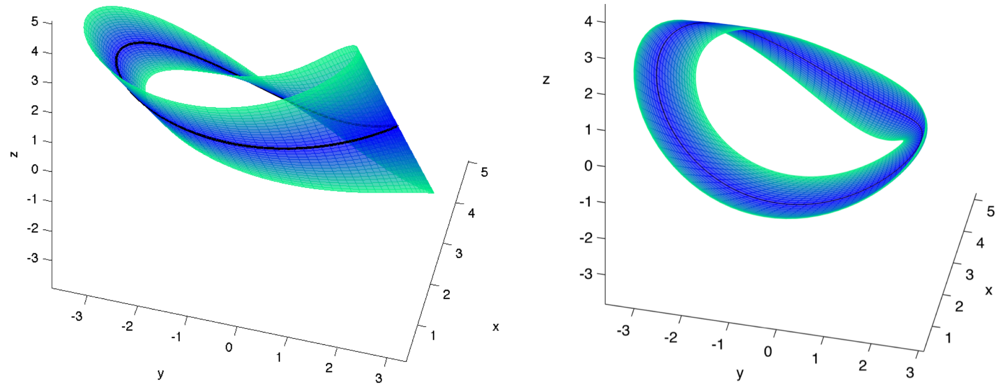

(a) (b)

Figure 8: (a) Stable and (b) unstable local manifolds of the periodic orbit for the Arneodo system. In this Figure the manifolds are computed using 20 Fourier and 10 Taylor modes.

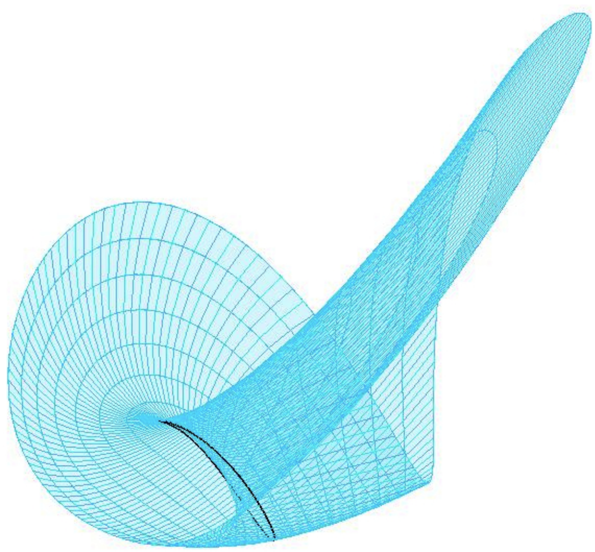

Figure 9: A larger local manifolds for the Arneodo manifold. This Figure illustrates the same manifold shown in Figure 3 however in this case the local approximation is taken to 45 Fourier modes and 40 Taylor modes. We see more nonlinear features of the manifold, but it is more difficult to see the Mobius Strip. Carefully following the boundary curve shows that there is still only one component of the boundary.

with the eigenvalues of R), and are given by $\lambda_1 = -0.16577$ and $\lambda_2 = -0.01044$. The orbit is stable and the corresponding Floquet multipliers are positive. Hence, the bundles are orientable. In this case computing the stable manifold of the orbit provides a trapping region for the orbit on which the dynamics are conjugate to linear. The stable manifold is illustrated in Figure 10.

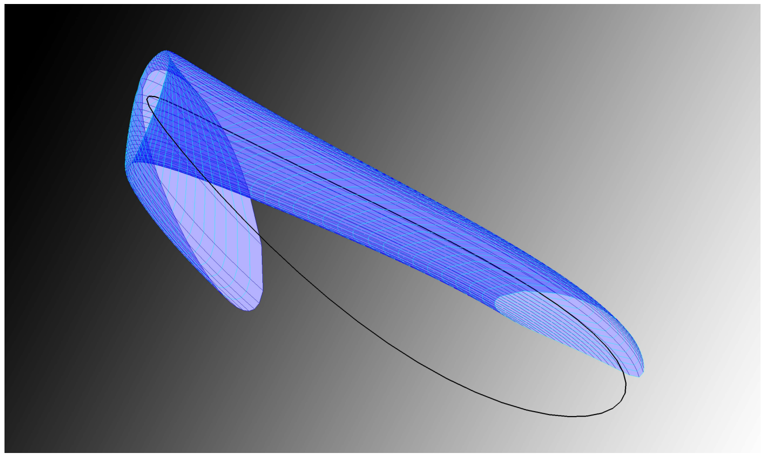

Figure 10: Boundary of a trapping region for the globally attracting periodic orbit of the Rössler system at $\lambda = 0.5$. The manifold is "cut away" to show the tubular quality of the trapping region. The trapping region is special in the sense that the dynamics in this tube is conjugate to the linear dynamics given by the linear flow (16). The conjugacy is given by the parameterization computed to Taylor order $N = 25$. The tube is the image of the Fourier-Taylor polynomial. No numerical integration is used to obtain this image.

A Truncation of the Kuramoto-Sivashinsky Equation

We conclude with a higher dimensional example which arises as a finite dimensional projection of a PDE. Consider the Kuramoto-Sivashinsky equation

$$\begin{aligned} u_t &= -u_{yy} - \rho u_{yyyy} + 2uu_y \\ u(t,y) &= u(t, y+2\pi), u(t,-y) = -u(t,y), \end{aligned} \tag{39}$$

which is a popular model to analyze weak turbulence or *spatiotemporal chaos* [36, 37].

We expand solutions of (39) using Fourier series as

$$u(t,y) = \sum_{n\in\mathbb{Z}} c_n(t) e^{iny}. \tag{40}$$

The functions $\xi_n(t)$ so that $c_n(t) = i\xi_n(t)$ solve the infinite system of real ODEs

$$\dot{\xi}_n = (n^2 - \rho n^4)\xi_n - n \sum_{n_1+n_2=n} \xi_{n_1}\xi_{n_2}, \tag{41}$$

where $\xi_{-n}(t) = -\xi_n(t)$, for all t, n. We consider a finite dimensional Galerkin projection of (41) of dimension $m = 10$

$$\dot{\xi}_n = (n^2 - \rho n^4)\xi_n - n \sum_{\substack{n_1+n_2=n \\ |k_i|\le 10}} \xi_{n_1}\xi_{n_2}, \qquad (n = 1, \dots, 10). \tag{42}$$

Hence, the periodic orbit Γ is stable. All associated Floquet multipliers are real and the associated eigenvector $w(\theta) = Q(\theta)w$ are not flipped over the interval $[0, \tau]$, and each associated bundle is orientable. Figure 11(a) shows the projection over the first three variables

(ξ_1, ξ_2, ξ_3) of the local stable manifold associated to the eigenvalue $\lambda_9 = -0.5730$, that is the *slow* stable manifold of the periodic orbit. This illustrates the fact that the Parameterization Method allows computation of invariant sub-manifolds of the full stable manifold associated with *slow* eigendirections. (Here we use the term "slow stable manifold" in the sense discussed in [5, 7]. Briefly, we are considering the manifold defined by conjugating the phase space dynamics near the periodic orbit to the linear dynamics associated with the slowest stable eigenvalue, in this case the eigenvalue $\lambda_9 = -0.5730$).

At $\rho = 0.11878$ there is a solution with period $\tau = 3.894911$. The eigenvalues of B result to be real: one of them is positive that is $\lambda_u = 1.135682$, while the rest are negative (i.e. stable). Hence there is one unstable direction. Figure 11(b) shows the local unstable manifold, again using the projection over the first three variables (ξ_1, ξ_2, ξ_3).

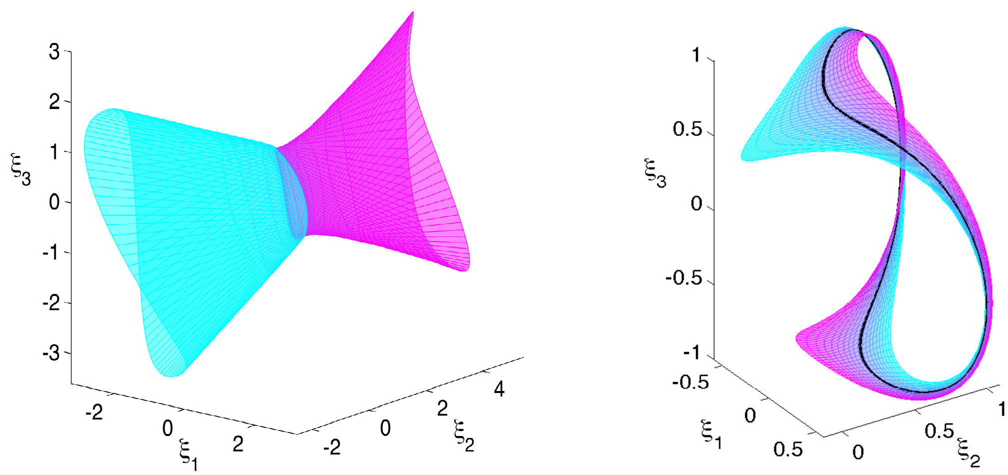

(a) (b)

Figure 11: (a) Local *slow* stable manifold associated with the eigenvalue $\lambda_9 = -0.5730$ of the periodic orbit at $\rho = 0.127$. (b) Local unstable manifold of a periodic orbit at $\rho = 0.11878$.

2.2.4 Validation

Validation of the manifolds can be achieved by considering the sequence space of Fourier-Taylor coefficients with an appropriate ℓ^1 norm. Then homological equations lead to the definition of a smooth map on this sequence space and the expansion of the covering map is equivalent to a zero of this map.

2.3 An infinite dimensional example: Spatially Inhomogeneous Fisher Equation

More recently the parameterization method is being extendedd for numerical computations and computer assisted proof in infinite dimensional systems. See for example the treatment for infinite dimensional maps in [38]. In this section we give a brief sketch of how the method can be implemented for studying unstable manifolds of parabolic PDEs. This unpublished material is part of a more general manuscript which is in preparation.

Consider the *spatially inhomogeneous Fisher equation* given by the partial differential equation

$$\frac{\partial}{\partial t}u(t,x) = \frac{\partial^2}{\partial x^2}u(t,x) + \mu u(t,x)(1 - c(x)u(t,x)), \qquad t \geq 0, \quad x \in [0,\pi] \tag{43}$$

subject to the Neumann boundary conditions

$$\frac{\partial}{\partial x}u(t,0) = \frac{\partial}{\partial x}u(t,\pi) = 0, \qquad \text{for all} \quad t \geq 0.$$

$$u_t = u_{xx} + \mu u(1 - cu) \tag{44}$$

subject to the Neumann boundary conditions

$$u_x(t,0) = u_x(t,2\pi) = 0 \quad \text{for all } t \geq 0,$$

and

$$u(0,x) = f(x)$$

with $f\colon [0,2\pi] \to \mathbb{R}$ a real analytic, 2π-periodic function of x. Here $c(x)$ is taken to be a real analytic function satisfying the boundary conditions. Denote by $\{a_n\}_{n=0}^\infty$ and $\{c_n\}_{n=0}^\infty$ the cosine series coefficients of f and c respectively and assume there is a $\nu > 1$ so that

$$|a_0| + 2\sum_{n=1}^\infty |a_n|\nu^n < \infty, \quad \text{and} \quad |c_0| + 2\sum_{n=1}^\infty |c_n|\nu^n < \infty.$$

Note that

$$u(t,x) = 0 \qquad \text{and} \qquad u(t,x) = c^{-1}(x),$$

are equilibria solutions of (44). We will assume that $c(x) \neq 0$.

More generally we look for solutions $u\colon \mathbb{R}^2 \to \mathbb{R}$ which are real analytic and 2π-periodic in x,

$$u(t,x) = u(t,x+2\pi)$$

for all t, x and which satisfy the boundary conditions. Note that if such a function is analytic then we automatically have that

$$\frac{\partial}{\partial x}u(t,x) = \frac{\partial}{\partial x}u(t,x+2\pi),$$

for all t, x.

Then the solutions can be represented as cosine series of the form

$$u(t,x) = a_0(t) + 2\sum_{n=1}^\infty a_n(t)\cos(nx).$$

Where $a_n(t)$ are analytic functions of time.

An equilibria of Equation (44) is constant in time and reduces to

$$u(x) = a_0 + 2\sum_{n=1}^\infty a_n \cos(nx),$$

so that $\{a_n\}_{n=0}^{\infty}$ is now constant real sequence.

Plugging the cosine series expansion of u into the PDE and matching like powers leads to the infinitely many algebraic equations

$$(\mu - n^2)a_n - \mu(c * a * a)_n = 0,$$

for $n \geq 0$. Here

$$(c * a * a)_n = \sum_{\substack{k_1+k_2+k_3=n \\ k_1,k_2,k_3 \in \mathbb{Z}}} c_{|k_1|} a_{|k_2|} a_{|k_3|}.$$

Define the operator F on ℓ^1_ν by

$$[F(a)]_n = (\mu - n^2)a_n - \mu(c * a * a)_n, \qquad n \in \mathbb{N} \tag{45}$$

A zero of F is equivalent to an equilibrium solution of the equation.

We want to compute the finite a parametrization of the finite dimensional unstable manifold of an equilibrium solution $\tilde{a}$, i.e. $F(\tilde{a}) = 0$. We build on the results of another CAP of this equilibrium, that is we assume to be given $\tilde{a}$ in the form $\tilde{a} = \hat{a} + a^{\infty}$ and also the linear data for $DF(\tilde{a})$ is given in the form

$$\begin{aligned} \lambda_i &= \hat{\lambda}_i + \delta_i \\ \xi_i &= \hat{\xi} + \xi^{\infty} \end{aligned} \tag{46}$$

In order to compute a parametrization of the unstable manifold $P : \mathbb{B}_1 \to l^1_\nu$ we solve the invariance equation

$$F(P(\theta)) = DP(\theta)\Lambda\theta \tag{47}$$

where Λ induces the flow $\Psi(t, \theta)$ on the unstable manifold via $\theta' = \Lambda\theta$, i.e $\Psi(t, \theta) = \exp(\Lambda t)\theta$. In particular $\lim_{t \to -\infty} \Psi(t, \theta) = 0$ for all $\theta \in \mathbb{B}_1$ and $\|\Psi(L, \theta)\| > 1$ for some $L = L(\theta)$.

Let us be precise on how (47) connects P and the unstable manifold. If we define the function

$$a(t) = P(\Psi(t, \theta))$$

for an arbitrary but fixed $\theta \in \mathbb{B}_1$, then the following statements are true:

1. $a(0) = P(\theta)$
2. $$a'(t) = DP(\Psi(t, \theta))\Lambda\Psi(t, \theta) = F(P(\Psi(t, \theta))) = F(a(t))$$
3. a is defined on $(-\infty, L(\theta))$, where $L(\theta) > 0$ might be 'small'

So if we find a solution P to the invariance equation then for every $\theta \in \mathbb{B}_1$ and $t \in (-\infty, L(\theta))$ the function

$$u(t, x) = a_0(t) + 2\sum_{n=1}^{\infty} a_n(t)\cos(nx).$$

defines an analytic solution (in space!!) to Fisher's equation.

2.3.1 One Dimensional Unstable Manifold for the Fisher PDE

The projected map on the space of Fourier-Taylor coefficients is given by:

$$\Phi(P)_{mn} := \begin{cases} p_{0n} - a_n & m = 0, n \geq 0 \\ p_{1n} - \xi_n & m = 1, n \geq 1 \\ (m\lambda + n^2 - \mu)p_{mn} + \mu \sum_{j=0}^{m} (c * p_{m-j} * p_j)_n & m \geq 2, n \geq 0. \end{cases}$$

The Fréchet derivative is

$$[D\Phi(P)H]_{mn} := \begin{cases} h_{0n} & m = 0, n \geq 0 \\ h_{1n} & m = 1, n \geq 1 \\ (m\lambda + n^2 - \mu)h_{mn} + 2\mu \sum_{j=0}^{m} (c * p_{m-j} * h_j)_n & m \geq 2, n \geq 0. \end{cases}$$

We truncate to

$$\Phi^{MN}(P^{MN})_{mn} := \begin{cases} p_{0n}^{MN} - \hat{a}_n^N & 0 \leq m, 0 \leq n \leq N \\ p_{1n}^{MN} - \hat{\xi}_n^N & m = 1, 0 \leq n \leq N \\ (m\lambda + n^2 - \mu)p_{mn} + \mu \sum_{j=0}^{m} (c^N * p_{m-j}^N * p_j^N)_n^N & 2 \leq m \leq M, 0 \leq n \leq N. \end{cases}$$

and have

$$[D\Phi^{MN}(P^{MN})H^{MN}]_{mn} := \begin{cases} h_{0n}^{MN} & 0 \leq m, 0 \leq n \leq N \\ h_{1n}^{MN} & m = 1, 0 \leq n \leq N \\ (m\lambda + n^2 - \mu)h_{mn} + 2\mu \sum_{j=0}^{m} (c^N * p_{m-j}^N * h_j^N)_n^N & 2 \leq m \leq M, 0 \leq n \leq N. \end{cases}$$

$\hat{P}^{MN} \in \mathbb{R}^{N+1}$ has $\Phi^{MN}(\hat{P}^{MN}) \approx 0$. Let $A^{MN} \approx D\Phi^{MN}(\hat{P}^{MN})^{-1}$. Define

$$[A^\dagger H]_{mn} :=:= \begin{cases} [D\Phi^{MN}(\hat{P}^{MN})H^{MN}]_{mn} & 0 \leq m \leq M, 0 \leq n \leq N \\ h_{mn} & m = 0, 1, n \geq N + 1 \\ (m\lambda + n^2 - \mu)h_{mn} & \text{otherwise.} \end{cases}$$

and

$$[AH]_{mn} := \begin{cases} [A^{MN}H^{MN}]_{mn} & 0 \leq m \leq M, 0 \leq n \leq N \\ h_{mn} & m = 0, 1, n \geq N + 1 \\ (m\lambda + n^2 - \mu)^{-1}h_{mn} & \text{otherwise.} \end{cases}$$

A Newton-like operator for the problem is

$$T(P) = P - A\Phi(P). \tag{48}$$

Then an analysis very similar to that discussed in [1] is used to validate the formal computation of the manifold.

3 Connecting Orbits and the Method of Projected Boundaries

We now return to the problem of connecting orbits for differential equations. We are ready to formulate the method of projected boundaries for differential equations.

3.1 Formulation for Flows

Let $f\colon \mathbb{R}^N \to \mathbb{R}^N$ be a smooth vector field and $p, q \in \mathbb{R}^N$ be hyperbolic equilibria for f. Suppose that $P\colon D^{m_p} \to \mathbb{R}^N$ and $Q\colon D^{m_q} \to \mathbb{R}^N$ are parameterizations of the local unstable and stable manifolds at p and q respectively. Just as in the case of maps, we say that there is a short connection from p to q (relative to P and Q) if the equation

$$P(\theta) - Q(\phi) = 0,$$

has a solution $(\theta_*, \phi_*) \in D^{m_p} \oplus D^{m_q}$. Note however that in the case of differential equations solutions of this equation cannot be isolated. This is because any infinitesimal flow of an intersection point is again a point of intersection. Then we look for a solution on a fixed sphere in the unstable parameter space.

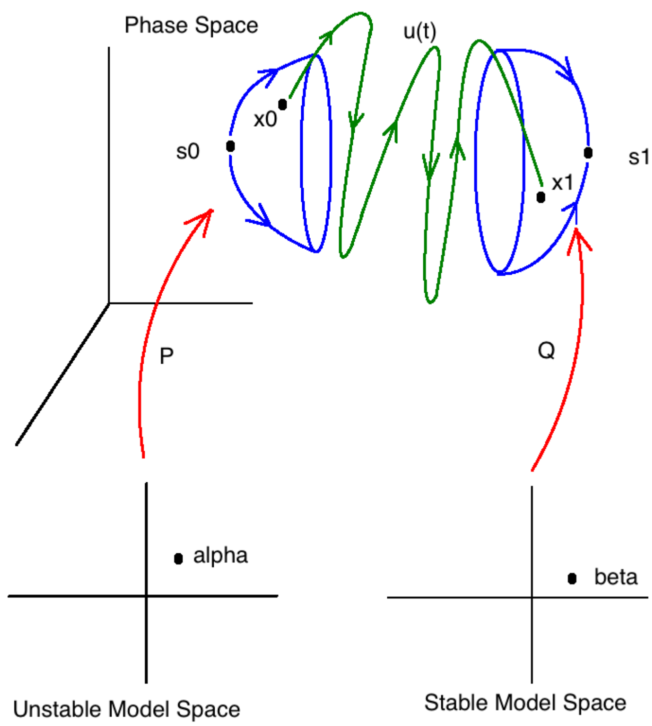

Figure 12: Projected boundaries for flows.

When the images of the local parameterizations P and Q do not intersect then the situation is a little more involved. Let $\Phi\colon \mathbb{R}^N \times \mathbb{R} \to \mathbb{R}^N$ denote the flow generated by f.

We define the map

$$F(\theta, \phi, T) = \Phi(P(\theta), T) - Q(\phi),$$

and seek θ_*, ϕ_*, T_* so that

$$F(\theta_*, \phi_*, T_*) = 0.$$

Then the orbit of $P(\theta_*)$ is heteroclinic from p to q. An equivalent operator not involving the flow Φ is given the integrated form, i.e. consider the operator $\mathcal{F}\colon \mathcal{X} \to \mathcal{X}$

$$\mathcal{F}(\alpha, \beta, T, x(t)) := \left(\begin{array}{c} Q(\phi(\beta)) - P(\theta(\alpha)) - \int_0^T f(x(\tau))\, d\tau \\ P(\theta(\alpha)) + \int_0^t f(x(\tau))\, d\tau - x(t) \end{array} \right),$$

where $\phi(\beta)$ and $\theta(\alpha)$ are parameterizations of spheres in the parameter spaces of the unstable and stable parameterizations. Then $\mathcal{F}$ maps the space

$$\mathcal{X} := \mathbb{R}^n \oplus C([0,T], \mathbb{R}^N),$$

to itself.

Discretization of $C([0,T], \mathbb{R}^n)$: The function space must be discretized in order to solve the problem numerically. In [39, 26] for example the function space is discretized using piecewise linear splines. Spectral approximation using Chebyshev series is used in [40, 41]. Chebyshev series are "Fourier series for boundary value problems" and are amenable to a sequence space a-posteriori analysis as discussed in the Lecture of J.B. van den Berg [1].

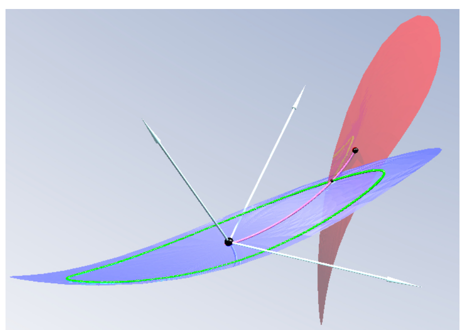

Figure 13: An illustration of a "short connection" for the Lorenz system. The green circle on the blue manifold illustrates the "phase condition" used to isolate the connecting orbit segment.

3.2 Example: Heteroclinic Connections, Patterns, and Traveling Waves

The following application appears in [40], and uses all of the techniques discussed above in order to solve an interesting pattern formation problem for PDEs. The pattern formation model

$$\partial_t \mathrm{U} = -(1+\Delta)^2 \mathrm{U} + \mu \mathrm{U} - \beta |\nabla \mathrm{U}|^2 - \mathrm{U}^3 \tag{49}$$

in the plane, i.e., $\mathrm{U} = \mathrm{U}(t,x) \in \mathbb{R}$, $t \geq 0$, $x \in \mathbb{R}^2$ was introduced in [42]. This equation generalizes the Swift-Hohenberg equation [43]. The additional term $\beta|\nabla \mathrm{U}|^2$, reminiscent

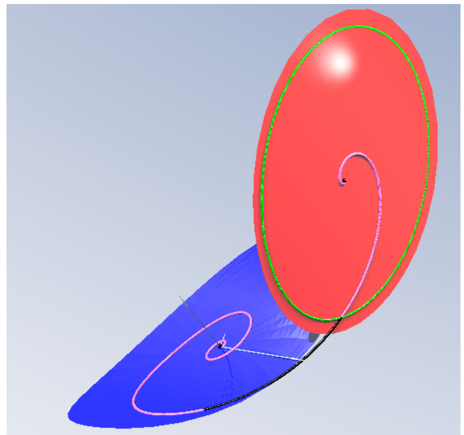

Figure 14: A long connection for Lorenz. Now the phase condition is the green circle on the red manifold. The black curve is the solution of the projected boundary value problem. The boundary value problem is discretized using piecewise linear splines. The pink curves are found using the conjugacy to the linear dynamics in the stable/unstable parameter spaces.

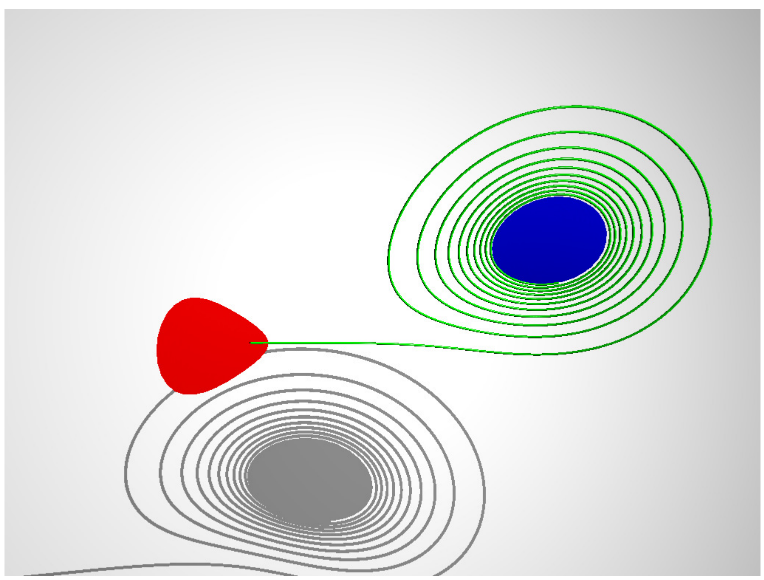

Figure 15: Long connection for the classic parameter values in Lorenz. The boundary value problem is discretized using Chebyshev series.

of the Kuramoto-Sivashinsky equation [36, 37], breaks the up-down symmetry $\mathrm{U} \mapsto -\mathrm{U}$ for $\beta \neq 0$. The Swift-Hohenberg equation acts as a phenomenological model for pattern formation in Rayleigh-Bénard convection, with $\beta \neq 0$ corresponding to a free boundary at the top of the convection cell, rather than a fixed one for the symmetric case $\beta = 0$ [44]. The parameter μ is related to the distance to the onset of convection rolls. For $\mu < 0$ the trivial equilibrium $\mathrm{U} \equiv 0$ is locally stable, whereas for $\mu > 0$ it is unstable.

Depending on the parameter values the dynamics generated by (49) exhibit a variety of patterns besides simple convection rolls (a stripe pattern); in particular, hexagonal spot patterns are observed. In [45] it is shown that stable hexagonal patterns with small amplitude can be found for $\beta < 0$ only. In [42] the interplay between hexagons and rolls near onset (small μ) is examined using a weakly nonlinear analysis. Introducing a small parameter $\epsilon > 0$, the parameters are scaled as

$$\mu = \epsilon^2 \tilde{\mu}, \qquad \beta = \epsilon \tilde{\beta}.$$

In the asymptotic regime $\epsilon \ll 1$, one can describe the roll and hexagonal patterns via amplitude equations. The seminal result in [42], based on spatial dynamics and geometric singular perturbation theory, is that heteroclinic solutions of the system

$$\begin{cases} 4B_1'' + \tilde{c}B_1' + \tilde{\mu}B_1 - \tilde{\beta}B_2^2 - 3B_1^3 - 12B_1B_2^2 = 0 \\ B_2'' + \tilde{c}B_2' + \tilde{\mu}B_2 - \tilde{\beta}B_1B_2 - 9B_1^3 - 6B_1^2B_2 = 0 \end{cases} \tag{50}$$

correspond to modulated front solutions, travelling at (rescaled) speed $\tilde{c}$, which corresponds to an asymptotically small velocity $\epsilon\tilde{c}$ in the original spatio-temporal variables. We note that the system (50) also shows up in the analysis of solidification fronts describing crystallization in soft-core fluids.

The variables B_1 and B_2 represent amplitudes of certain wave modes (slowly varying in the original variables). We refer to [42] for the details and the rigorous justification of the derivation. The dynamical system (50) has up to seven stationary points:

$$\begin{array}{ll} (B_1, B_2) = (0, 0) & \text{trivial state} \\ (B_1, B_2) = (B_{\text{rolls}}, 0) & \text{“positive” rolls} \\ (B_1, B_2) = (-B_{\text{rolls}}, 0) & \text{“negative” rolls} \\ (B_1, B_2) = (B_{\text{hex}}^+, B_{\text{hex}}^+) & \text{hexagons} \\ (B_1, B_2) = (B_{\text{hex}}^-, B_{\text{hex}}^-) & \text{“false” hexagons} \\ (B_1, B_2) = (-\tilde{\beta}/3, B_{\text{mm}}^\pm) & \text{two “mixed mode” states.} \end{array} \tag{51}$$

Here $B_{\text{rolls}} = \sqrt{\tilde{\mu}/3}$ and $B_{\text{hex}}^\pm = \frac{-\tilde{\beta}\pm\sqrt{\tilde{\beta}^2+60\tilde{\mu}}}{30}$ and $B_{\text{mm}}^\pm = \pm\frac{1}{3}\sqrt{\tilde{\mu} - \tilde{\beta}^2/3}$. Due to symmetry, there are two equilibria corresponding to rolls. We refer to [42] for a full discussion of all states and their stability properties. In this paper we consider the interplay between hexagons and rolls (both positive and negative).

While the weakly nonlinear analysis in [42] provided a vast reduction in complexity from (49) to (50), one outstanding issue remained: the heteroclinic solutions are difficult to analyse rigorously due to the nonlinear nature of the equations (50). In the limit $\tilde{c} \to \infty$ various connections could be found through a further asymptotic reduction [42], but for finite wave speeds the analysis of (50) was out of reach. In the present paper we introduce v a computer-assisted, rigorous method for finding heteroclinic solutions for $\tilde{c} = 0$, i.e. standing waves. In particular we find connections between hexagons and rolls with *zero* propagation speed, i.e., the two patterns coexist.

The system (50) is gradient-like for $\tilde{c} \neq 0$, while it is Hamiltonian for $\tilde{c} = 0$. Hence, for hexagons and rolls to coexist their free energy must be equal, a situation that occurs when $\tilde{\mu} = \frac{7+3\sqrt{6}}{30}\tilde{\beta}^2$. We prove the following theorem, which settles the conjecture in [42] about the coexistence of hexagons and rolls:

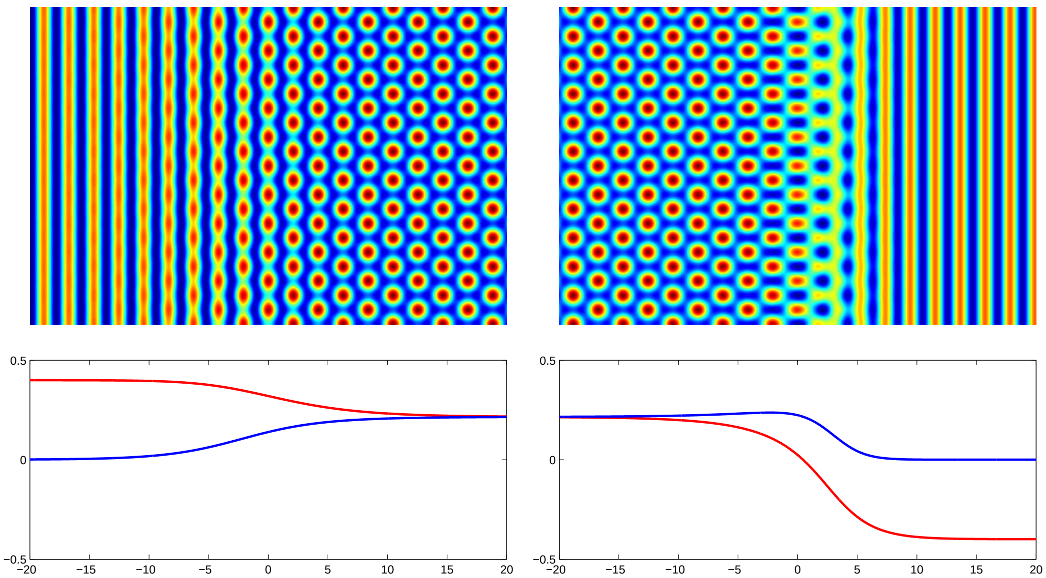

Figure 16: At the bottom are graphs of B_1 (red) and B_2 (blue) representing heteroclinic solutions of (50) that connect the hexagon state to the positive rolls (on the left) and negative rolls (and the right). The parameter values are $\tilde{c} = 0$, $\tilde{\mu} = \frac{7+3\sqrt{6}}{30}$ and $\tilde{\beta} = 1$, corresponding to the assumptions in Theorem 3.1. At the top we illustrate the corresponding stationary patterns of (49). We note that the two phase transitions from rolls to hexagons have distinctive features. On the left, the stripes ("positive" rolls) undergo pearling, which gradually leads to separation into spots (hexagons). On the right, the stripes ("negative" rolls) develop transverse waves, which break up into a block structure that then transforms into hexagonal spots. The figures of the patterns at the top were made using $\epsilon = \frac{1}{3}$. For smaller ϵ the transition between the two states is more gradual.

Theorem 3.1. *For parameter values $\tilde{\mu} = \frac{7+3\sqrt{6}}{30}\tilde{\beta}^2$ and $\tilde{c} = 0$ there exists a heteroclinic orbit of* (50) *between the hexagons and positive rolls, see* (51)*, as well as a heteroclinic orbit between the hexagons and negative rolls.*

The heteroclinic solutions are depicted in Figure 16, together with the corresponding patterns of the PDE (49). These orbits thus represent two types of stationary domain walls between hexagons and rolls (spots and stripes). While each heteroclinic connection exists on a parabola in the $(\tilde{\beta}, \tilde{\mu})$ parameter plane, a parameter scaling reduces this to a single connecting orbit.

The problem is solved using a scheme very similar to the one illustrated above for the Lorenz system. So, an approximate solution u_{num}, obtained through a numerical calculation. We then construct an operator which has as its fixed points the heteroclinic solutions, and we set out to prove that this operator is a contraction mapping on a small ball around u_{num} in an appropriate Banach space. The ball should be small enough for the estimates to be sufficiently strong to prove contraction, but large enough to include both u_{num} (the center of the ball) and the solution (the fixed point). Qualitatively, considering the numerical approximations of solutions depicted as graphs in Figure 16, we can choose the radius of the ball so small that the solution is guaranteed to lie within the thickness of the lines.

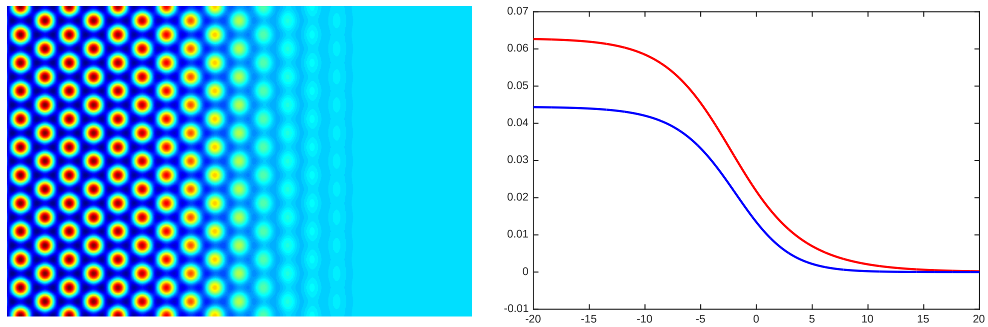

Figure 17: Left: co-existing hexagonal and trivial patterns for $\beta = 1$ and $\mu = -\frac{2}{135}$. Right: corresponding connecting orbit with u and v components in red and blue, respectively.

Note: the rigorous justification in [42] of the link between the PDE (49) and the ODE system (50) focuses on the case of nonzero propagation speed. The case of stationary fronts is only briefly mentioned in [42], since in that case the ODEs can be found more directly by a reduction to a spatial center manifold. In both the zero and nonzero speed setting, the rigorous derivation of (50) relies on a (weakly) nonlinear analysis to justify that one may ignore higher order terms in ϵ. Reciprocally, a heteroclinic solution of (50) is only guaranteed to survive in the full PDE system for small $\epsilon > 0$, if the orbit is a transversal intersection of stable and unstable manifolds. This is clearly *not* the case in (50) for $\tilde{c} = 0$, since the system is Hamiltonian. On the other hand, one should be able to exploit the "robustness" of the solution, which is a by-product of the contraction argument, to justify rigorously that existence of the front extends to the full system for small $\epsilon > 0$. However, since stationary coexistence (i.e. a pinned front) is a co-dimension one phenomenon, this needs to be viewed in the context of embedding the $\tilde{c} = 0$ case into a one parameter family of heteroclinic orbits with wave speed $\tilde{c} = \tilde{c}(\gamma)$. In that setting transversality is recovered.

Finally, to find a connection for $\tilde{c} = 0$ between the hexagons and the trivial state (the appropriate parameter value for coexistence is $\tilde{\mu} = -\frac{2}{135}\tilde{\beta}^2$), one needs to deal with resonances between eigenvalues in the spectrum of the trivial state. The resonance problem is treated in [23], and there the interested reader can find the computer assisted proof of the connection between the hexagons and the trivial state.

3.3 Example: Homoclinic Tangle for Periodic Orbits in the Lorenz and Kuromoto Systems

The method of projected boundaries is extended to connecting orbits between periodic orbits simply by replacing the parameterizations of the local stable/unstable manifolds of the fixed points by the parameterizations of the local stable/unstable manifolds of the periodic orbits. Details are found in [32], and some numerically computed connecting orbits are illustrated in the figures.

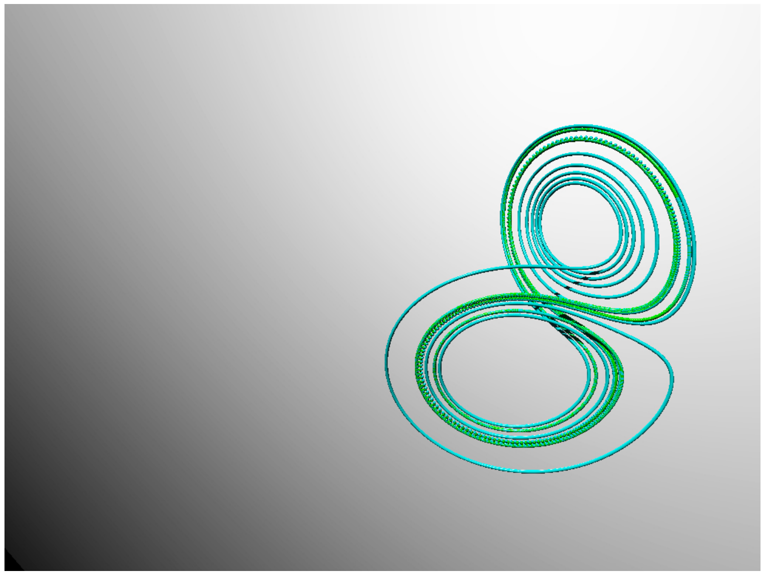

Figure 18: Homoclinic connection for a periodic orbit in the attractor of the Lorenz systems.

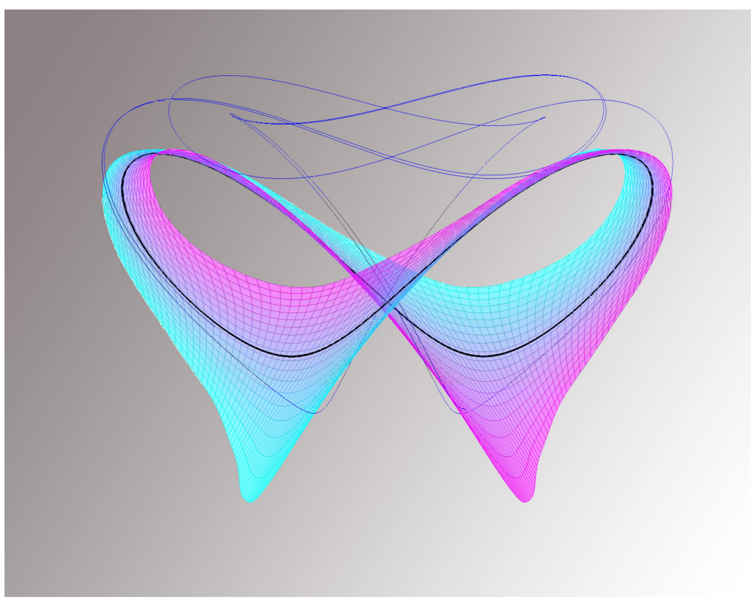

Figure 19: Homoclinic connection for a periodic orbit of the Kuramoto-Shivisinsky PDE, truncated to ten spatial modes.

3.4 The Future...

References

[1] J. B. Van den Berg. Introduction: general setup and an example that forces chaos. *(AMS short course notes)*, 2015.

[2] W.-J. Beyn. The numerical computation of connecting orbits in dynamical systems. *IMA J. Numer. Anal.*, 10(3):379–405, 1990.

[3] J. D. Mireles James and Konstantin Mischaikow. Rigorous a posteriori computation of (un)stable manifolds and connecting orbits for analytic maps. *SIAM J. Appl. Dyn. Syst.*, 12(2):957–1006, 2013.

[4] S. Smale. Differentiable dynamical systems. *Bull. Amer. Math. Soc.*, 73:747–817, 1967.

[5] X. Cabré, E. Fontich, and R. de la Llave. The parameterization method for invariant manifolds. I. Manifolds associated to non-resonant subspaces. *Indiana Univ. Math. J.*, 52(2):283–328, 2003.

[6] X. Cabré, E. Fontich, and R. de la Llave. The parameterization method for invariant manifolds. II. Regularity with respect to parameters. *Indiana Univ. Math. J.*, 52(2):329–360, 2003.

[7] X. Cabré, E. Fontich, and R. de la Llave. The parameterization method for invariant manifolds. III. Overview and applications. *J. Differential Equations*, 218(2):444–515, 2005.

[8] A. Haro and R. de la Llave. A parameterization method for the computation of invariant tori and their whiskers in quasi-periodic maps: explorations and mechanisms for the breakdown of hyperbolicity. *SIAM J. Appl. Dyn. Syst.*, 6(1):142–207 (electronic), 2007.

[9] À. Haro and R. de la Llave. A parameterization method for the computation of invariant tori and their whiskers in quasi-periodic maps: numerical algorithms. *Discrete Contin. Dyn. Syst. Ser. B*, 6(6):1261–1300 (electronic), 2006.

[10] A. Haro and R. de la Llave. A parameterization method for the computation of invariant tori and their whiskers in quasi-periodic maps: rigorous results. *J. Differential Equations*, 228(2):530–579, 2006.

[11] C. Simo. On the Analytical and Numerical Approximation of Invariant Manifolds. In D. Benest and C. Froeschle, editors, *Modern Methods in Celestial Mechanics, Comptes Rendus de la 13ieme Ecole Printemps d'Astrophysique de Goutelas (France), 24-29 Avril, 1989. Edited by Daniel Benest and Claude Froeschle. Gif-sur-Yvette: Editions Frontieres, 1990., p.285*, page 285, 1990.

[12] Oscar E. Lanford, III. A computer-assisted proof of the Feigenbaum conjectures. *Bull. Amer. Math. Soc. (N.S.)*, 6(3):427–434, 1982.

[13] J.-P. Eckmann, H. Koch, and P. Wittwer. A computer-assisted proof of universality for area-preserving maps. *Mem. Amer. Math. Soc.*, 47(289):vi+122, 1984.

[14] Warwick Tucker. The Lorenz attractor exists. *C. R. Acad. Sci. Paris Sér. I Math.*, 328(12):1197–1202, 1999.

[15] Warwick Tucker. A rigorous ODE Solver and Smale's 14th Problem. *Foundations of Computational Mathematics*, 2(1):53–117–117, 2002-12-21.

[16] R. de la Llave, A. González, À. Jorba, and J. Villanueva. KAM theory without action-angle variables. *Nonlinearity*, 18(2):855–895, 2005.

[17] Renato C. Calleja, Alessandra Celletti, and Rafael de la Llave. A KAM theory for conformally symplectic systems: efficient algorithms and their validation. *J. Differential Equations*, 255(5):978–1049, 2013.

[18] Gemma Huguet, Rafael de la Llave, and Yannick Sire. Computation of whiskered invariant tori and their associated manifolds: new fast algorithms. *Discrete Contin. Dyn. Syst.*, 32(4):1309–1353, 2012.

[19] Gemma Huguet and Rafael de la Llave. Computation of limit cycles and their isochrons: fast algorithms and their convergence. *SIAM J. Appl. Dyn. Syst.*, 12(4):1763–1802, 2013.

[20] Ernest Fontich, Rafael de la Llave, and Yannick Sire. A method for the study of whiskered quasi-periodic and almost-periodic solutions in finite and infinite dimensional Hamiltonian systems. *Electron. Res. Announc. Math. Sci.*, 16:9–22, 2009.

[21] Rafael de la Llave and Jason D. Mireles James. Parameterization of invariant manifolds by reducibility for volume preserving and symplectic maps. *Discrete Contin. Dyn. Syst.*, 32(12):4321–4360, 2012.

[22] A. Haro, M. Canadell, J-LL. Figueras, A. Luque, and J-M. Mondelo. *The parameterization method for invariant manifolds: from theory to effective computations*, volume -. 2014. Preprint `http://www.maia.ub.es/~alex`.

[23] J. B. Van den Berg, J. D. Mireles James, and Christian Reinhardt. Computing (un)stable manifolds with validated error bounds: non-resonant and resonant spectra. *(Submitted)*.

[24] M. Breden, J.P. Lessard, and J.D. Mireles James. Computation of maximal local (un)stable manifold patches by the parameterization method. *(Submitted)*.

[25] J. D. Mireles James and Hector Lomelí. Computation of heteroclinic arcs with application to the volume preserving Hénon family. *SIAM J. Appl. Dyn. Syst.*, 9(3):919–953, 2010.

[26] Jean-Philippe Lessard, Jason D. Mireles James, and Christian Reinhardt. Computer assisted proof of transverse saddle-to-saddle connecting orbits for first order vector fields. *J. Dynam. Differential Equations*, 26(2):267–313, 2014.

[27] Donald E. Knuth. *The art of computer programming. Vol. 2*. Addison-Wesley Publishing Co., Reading, Mass., second edition, 1981. Seminumerical algorithms, Addison-Wesley Series in Computer Science and Information Processing.

[28] A. Haro. Automatic differentiation methods in computational dynamical systems: Invariant manifolds and normal forms of vector fields at fixed points. *Manuscript*.

[29] Àngel Jorba and Maorong Zou. A software package for the numerical integration of ODEs by means of high-order Taylor methods. *Experiment. Math.*, 14(1):99–117, 2005.

[30] Warwick Tucker. *Validated numerics*. Princeton University Press, Princeton, NJ, 2011. A short introduction to rigorous computations.

[31] Julian Ransford, J.P. Lessard, and J. D. Mireles James. Automatic differentiation for fourier series and the radii polynomial approach. *(Submitted)*.

[32] Roberto Castelli, Jean-Philippe Lessard, and J. D. Mireles James. Parameterization of invariant manifolds for periodic orbits i: Efficient numerics via the floquet normal form. *SIAM Journal on Applied Dynamical Systems*, 14(1):132–167, 2015.

[33] Carmen Chicone. *Ordinary differential equations with applications*, volume 34 of *Texts in Applied Mathematics*. Springer, New York, second edition, 2006.

[34] J. D. Mireles James. Quadratic volume-preserving maps: (un)stable manifolds, hyperbolic dynamics, and vortex-bubble bifurcations. *J. Nonlinear Sci.*, 23(4):585–615, 2013.

[35] Antoni Guillamon and Gemma Huguet. A computational and geometric approach to phase resetting curves and surfaces. *SIAM J. Appl. Dyn. Syst.*, 8(3):1005–1042, 2009.

[36] Y. Kuramoto and T. Tsuzuki. Persistent propagation of concentration waves in dissipative media far from thermal equilibrium. *Prog. Theor. Phys.*, 55(365), 1976.

[37] G. I. Sivashinsky. Nonlinear analysis of hydrodynamic instability in laminar flames. I. Derivation of basic equations. *Acta Astronaut.*, 4(11-12):1177–1206, 1977.

[38] J. D. Mireles James. Fourier-taylor approximation of unstable manifolds for compact maps: numerical implementation and computer assisted error bounds. *(submitted).*

[39] Jan Bouwe van den Berg, Jason D. Mireles-James, Jean-Philippe Lessard, and Konstantin Mischaikow. Rigorous numerics for symmetric connecting orbits: even homoclinics of the Gray-Scott equation. *SIAM J. Math. Anal.*, 43(4):1557–1594, 2011.

[40] Jan Bouwe van den Berg, Andréa Deschênes, Jean-Philippe Lessard, and Jason D. Mireles James. Coexistence of hexagons and rolls. Preprint, 2014.

[41] Jean-Philippe Lessard and Christian Reinhardt. Rigorous Numerics for Nonlinear Differential Equations Using Chebyshev Series. *SIAM J. Numer. Anal.*, 52(1):1–22, 2014.

[42] Arjen Doelman, Björn Sandstede, Arnd Scheel, and Guido Schneider. Propagation of hexagonal patterns near onset. *European J. Appl. Math.*, 14(1):85–110, 2003.

[43] J.B. Swift and P.C. Hohenberg. Hydrodynamic fluctuations at the convective instability. *Phys. Rev. A*, 15(1), 1977.

[44] Guoguang Lin, Hongjun Gao, Jinqiao Duan, and Vincent J. Ervin. Asymptotic dynamical difference between the nonlocal and local Swift-Hohenberg models. *J. Math. Phys.*, 41(4):2077–2089, 2000.

[45] Martin Golubitsky, Ian Stewart, and David G. Schaeffer. *Singularities and groups in bifurcation theory. Vol. II*, volume 69 of *Applied Mathematical Sciences*. Springer-Verlag, New York, 1988.